IEEE Access
Multidisciplinary | Rapid Review | Open Access Journal

Received September 5, 2019, accepted October 1, 2019, date of publication October 4, 2019, date of current version October 25, 2019.

Digital Object Identifier 10.1109/ACCESS.2019.2945527

A New Automatic Identification Method of Heart Failure Using Improved Support Vector Machine Based on Duality Optimization Technique

GAMAL G. N. GEWEID[1,2], (Member, IEEE), AND MAHMOUD A. ABDALLAH[3], (Member, IEEE)

[1]Electrical Engineering Department, School of Electrical Engineering and Computer Science, University of North Dakota, Grand Forks, ND 58202, USA
[2]Electrical Engineering Department, Benha Faculty of Engineering, Benha University, Benha 13511, Egypt
[3]Manufacturing Engineering Department, Central State University, Wilberforce, OH 45384, USA

Corresponding author: Gamal G. N. Geweid (gamal.geweid@und.edu)

ABSTRACT Currently, Heart failure disease is considered a multifaceted clinical disease affecting millions of people worldwide. Hospitals and cardiac centers rely heavily on ECG as a regular tool for evaluating and diagnosing Heart failure disease as an initial stage. The process of Heart failure disease identification from the ECG signal aims to reduce the time of the diagnostic process for patients with heart failure and to improve the outcomes of the detection process applied to these patients. The information acquired from the ECG signal simplifies the laboratory evaluation and other traditional diagnosis methods to evaluate and diagnose Heart failure disease. Unluckily, the problem of segmentation of the ECG signal is complicated because of similarities in time interval and amplitude between several ECG signal as well as the presence of noise in ECG signals. Most cardiologists use the ECG signal to identify Heart failure disease and their decision depends on the identification process, to determine whether surgery or medical treatment is required. This paper offers a new identification technique to overcome the current problems, such as overlapping in heart rate duration from the time interval from one PQRST wave to the next. In this study, the aim is to develop a new automatic method using improved support vector machine to diagnosis HFD from ECG signals. This is particularly relevant to ECG signals for the diagnosis of HFD as the first step to treatment and care of patients in general and specifically those with early heart disease to increase their overall survival. This paper outlines a hybrid approach of dual SVM and nonparametric algorithm to spot HFD in ECG signals leading to increase reliability and accuracy of identification and diagnosis of heart failure classes in the early stages using the proposed algorithm. The nonparametric algorithm is used to train SVM and its dual to get two models of SVM. The dual problem gives a different view that is better and sometimes simpler than the original problem. This feature is used to detect Heart failure disease in ECG signals by comparing the outputs of SVM model and those of dual SVM model. Experiments show that the hybrid approach produces good results, is more efficient and increases accuracy of Heart failure disease detection with an acceptable accuracy of 94.97% when compared with other algorithms to which the paper refers to. This is especially noted in patients with multiple diseases who were not initially identified as heart failure.

INDEX TERMS Heart failure disease (HFD), ECG, support vector machine (SVM), nonparametric algorithm, duality.

I. INTRODUCTION

Heart failure disease (HFD), with the highest prevalence worldwide, is of multi-factorial pathology. Cardiac output is reduced as a result of change in mechanical properties and altered cardiac electrical activity in some cases [1], [2].

The associate editor coordinating the review of this manuscript and approving it for publication was Hamed Azami.

In early stages of HFD there are a variety of neurohormonal regulatory mechanisms that are triggered [3]. Although these compensatory mechanisms can make up for consequences of HFD in the short-term, they can lead to dyspnea on exertion, pulmonary and peripheral edema, remodeling of the heart and accentuate ventricular dysfunction which can cause permanent changes in preload and afterload [4], [5]. Many treatment options are offered to patient with HFD such

as life style changes, medications or implantable devices such as a pacemaker or defibrillator [4]. Ensuring follow up in this population is a major concern given hospitalization due to acute decompensation of HFD is the leading cause of health care expenditure [5]. Studies and statistics found that heart diseases are the most important problems facing people especially HFD. Like other diseases, early detection and diagnosis of cardiac disease is the first step for treatment and care [1], [6].

HFD is now an emerging disorder for diseases such as heart disease, insomnia, hypertension as well as other diseases [7]. Detection of HFD on Electrocardiogram (ECG) is done through detection of variations in heart beat duration from the time interval from one PQRST wave to the next PQRST wave [8]. Changes in the cardiovascular system during HFD episodes lead to bradycardia during breathing episodes and tachycardia upon cessation of the breathing episode [9]. P, Q, R, S, and T waves stand for heart action, where P-wave defines the depolarization of the atria, Q-wave defines the deactivation of the anteroseptal region of the ventricular myocardium, R-wave defines the depolarization of the ventricular myocardium, S-wave defines the activation of the posterior basal portion of the ventricles, and T-wave defines the rapid ventricular repolarization.

There are many algorithms that can be used for heart failure identification from the ECG signal such as support vector machine (SVM) toolset based on LIBSVM [10], SVM based on a sequential minimum optimization (SMO) and artificial neural network (ANN) for heart disease classification [11], multilayer perceptron neural network (MLPNN), learning vector quantization neural network (LVQNN), multilayer perceptron (MLP) [12], SVM with sequential minimal optimization algorithm and the radial basis function (RBF) network structure based on Orthogonal Least Square (OLS) [13].

Chen *et al.* [10] have used information from patients with grouped heart failure (HF) and related medications as traits for training and predicting the type of patient with unknown HF from their prescription medications. After a ten-fold cross validation by choosing the radial basis function of SVM, with a cost of 0.075, gamma of 0.5, they got an average precision rate of 75.26%. These constraints were automatically nominated using the self-learning module in LIBSVM. Based on their paper results of the tests of all the medical documents compiled, they have summarized that the deceased patients tend to have decreasing Exposure Factor (EF) differences in comparison with all the living patients with heart failure [10].

Compared to other types of patients with heart failure, patients with systolic heart failure and heart valve failure have greater differences in EF over the last four years. They also stated that, the method predicted the years of survival and the life expectancy of the patient with accuracy rates between 80% and 87% under different parameter settings [10]. The LIBSVM method has used different functions applied to the ECG signal to predict the type of patient with unknown HF from their prescription medications. These functions include an initialization function which is used to acquire an ECG signal using a bio-potential amplifier and then displays it using ECG instrumentation, a preprocessing function, an analyzing function to analyse ECG signal, and a classifier function to classify the heart failure disease. This paper used feature analysis on heart failure classes and associated medications using SVM TOOLSET based on LIBSVM as presented in [10] to classify several categories of patients with heart failure.

Classification of HFD using SVM based on SMO and ANN method is presented in [11]. This method provides a support system for the medical decision for the classification of heart diseases. Deepti Vadicherla and Sheetal Sonawane have classified the data into 2 classes (positive one for absence of disease, and negative one for presence of disease) using SVM based on SMO process and ANN. They have compared between the results of classifiers SVM and ANN. The SVM classifier uses previously processed data as input to SMO for improved results with high accuracy. According to the mission of solving the problem of classification of heart disease and use the statistical methods in feature extraction stage, the results of SVM classifier based on SMO is greater than ANN [11].

Lewicke *et al.* [12] used MLPNN, LVQNN, and SVMs to classify sleep versus wake from ECG signal [12]. In general, the assessment of sleep status is a time consuming task and sleep states are derived manually from several biological signals. The method was applied with eight-hours concurrent ECG and poly-somno-gram (PSG) sleep counts of 190 newborns who participated in the collaborative monitoring of child monitors (CHIME) study [12]. As a classifier, the LVQNN, the multilayer MLPNN, and (SVM) were analyzed. After systematically rejecting the difficulty of classifying the segments of CHIME, the methods can achieve a correct classification of 85% to 87% while rejecting only 30% of the records for CHIME. If rejected, the accuracy increases by approximately 8% compared to a method without elimination. In addition, the influence of PSG epochs with indeterminate states is analyzed [12].

Ghumbre, Shashikant, Chetan Patil, and Ashok Ghatol used the SVM in heart disease diagnosis [13]. In this work, the use of artificial intelligence in the diagnosis of typical cardiac disorder was investigated. They have presented an intelligent SVM based on a system with a radial basis function network for diagnostics. A clinical expert system based on symptoms is used to decide what type of cardiac disorder a patient may experience, be it a heart attack or not. The SVM based on a SMO algorithm is applied to the Indian patient data sets. Then, the structure of the RBF network trained by the OLS is applied to the same set of predictive data. The results show that the SVM based on SMO can be used successfully to diagnose cardiac disorder [12]. Hammad *et al.* [14] introduced a classifier to detect abnormal heart conditions based on ECG signal characteristics. In their method, the proposed classifier is created by extracting the major features from de-noised ECG signals. They conducted comparative studies

of NN, SVM, KNN with their method to classify the ECG signals [14].

Amrani *et al.* [15] used multi-canonical correlation analysis (MCCA) method to detect arrhythmias in ECG signals. The method is based on very deep feature extraction and fusion. They also applied the Q-Gaussian (QG) multiclass SVM to classify arrhythmias from ECG signals [15].

Hammad *et al.* [16] introduced a classifier based on two-dimensional ECG feature extraction and convolutional neural network (CNN). In this method, a real-time authentication system is used to extract the main features from the ECG signals that have negative peaks, high-grade noise and baseline drift [16].

Analysis of the data would be useful to develop a better understanding of HFD and its leading events to improve detection early on. Several lumped-parameter models of the cardiovascular system have been proposed in literature but very few provide both short-term and long-term cardiovascular regulations as well as multiorgan regulation in order to fully analyze HFD. In the proposed method, multiorgan representation of the chorionic villus sampling (CVS) and its regulation can be used to analyze events over different time scales ranging from seconds to months. Most current HFD diagnosis methods are not included in the identification models which are a major limitation in the study of HFD because of systolic and diastolic characteristics of HFD cannot be represented. In addition to arterial pressure derivatives cannot be simulated and representation of short term regulatory loops require pulsatile variables [7], [8]. Arterial pressure is associated with heart rate variability (HRV) leading to changing R-R, QRST durations in an ECG [8]. This research uses datasets with about 82% of subjects have high blood pressure (hypertension).

In this work, a population of patients with heart failure using ECG signal analysis was studied. This paper focuses on a multivariate analysis of a set of physiological parameters that were applied to P-QRS-T wave for the early detection of HFD.

A new hybrid approach is presented to detect Cardiac disease from ECG signal. The proposed approach provides HFD detection with high accuracy to increase survival rate and save many people without the risk of having heart attack and/or immediate stroke. The approach merely requires good PC or laptop set to detect the cardiac disease especially HFD from Electrocardiogram signal processing. This paper introduces a new method for predicting, identifying the type of patient with unknown HF from their ECG signals only. The proposed approach is suitable for developing regions such as the Middle-east, Africa, and Asia. A hybrid approach is developed to detect HFD disease using Improved Support Vector Machine (ISVM) based on Duality Optimization (DO) technique.

This paper suggests the use of combination of improved support vector machine and duality optimization to find P-QRS-T peaks and troughs of ECG signals to discriminate the normal and disease-related conditions. In this method, ECG waveform is divided into five waves (P, Q, R, S, and T) based on time interval and amplitude for each wave. It is also supposed that the three areas (P-QRS-T) are dissimilar in that they take different probability amplitude functions for each + ve peak value and –ve peak value of the ECG signal and that the time intervals borderline of the P-QRS-T waves inside the three segment areas are distributed and divided in an identical way.

Five features are presented in the proposed approach using ISVM to better read the ECG signal. Using DO form of SVM with the original one to give a complete view of the ECG signal while using nonparametric algorithm to train SVM and its dual and provide a normal ECG for SVM to avoid the noise. The dual form is used because the dual can be helpful for sensitivity ± peak-value and time interval analysis. Sometimes finding an initial feasible solution to the dual is much easier than finding one for the primal. The dual variables give the shadow prices (dual price) for the primal constraints. The importance of duality for the heart failure classification process is detecting the PQRST amplitudes in an ECG signal with more accuracy than other techniques because the mathematical optimization theory is based on the primal constraints (original function and dual function). Sometimes the dual is just easier to solve) A problem with many constraints and few variables can be converted into one with few constraints and many variables). Many lemmas and theorems indicate the relations between the primal problem and dual one [8]. The most important theorems are the weak duality theory and the strong duality theory which are presented below. The proposed approach is an attempt to examine ECG signal with a view to spotting any abnormal signs in the ECG especially HFD.

The advantage of this method is applicable to ECG signals with several amplitude and duration of the P-QRS-T waves, differentiating between normal and abnormal ECG signals based on heart rate duration from the time interval from one PQRST wave to the next PQRST wave, predicting and diagnosing the HF from an ECG signal only. Level set methods can easily handle peak-value and time interval changes of the developing contour such as singularities on the curve due to sharp corners, splitting and merging. Later, the shared data and energy function as multiphase area were calculated. The gradient flow computation of the ECG signal ± peak-value and time interval borderline were checked for location whether it is inside or outside. Low frequency noise can be dealt with by involving a coarse to fine multiscale procedure, which promises improvements of the ECG signal. A Gaussian conditional field is built to obtain the underlying clean ECG signal from the noisy input. After these steps are taken, the segmented P-QRS-T wave is obtained.

This paper is organized as follows: Section II presents the Human Heart system. Section III shows Electrocardiogram signal segmentation using information-theoretic, problem illustration and ECG signal pre-processing. Section IV includes the identification hybrid approach, SVM, dual SVM, the theorems and the relationships between them.

Section V illustrates the HFD identification performance. The experimental results are presented in section VI by using test ECG waveforms. Section VII presents the comparative analysis and case study. Section VIII illustrates the performance evaluation and cross-validation. Finally, Section IX concludes the paper.

II. HUMAN HEART SYSTEM

In the human heart system, electrical activity of the heart can be recorded by ECG with distinct waveforms via skin electrodes. It is a non-invasive technique that reflects cardiac health, heart beat and heart rate for identification of heart disease. Most human body cells are not in direct contact with the outer location. Therefore, they rely on the cardiovascular system to serve as a transport provision for them.

In the cardiovascular system, there are two types of fluids that flow through it. The first one is blood, in this type of fluid, the heart and blood vessels form the circulatory system. The second one is lymph, in this type of fluid; the lymph nodes and the lymphatic vessels form the lymphatic structure. The vascular system and the lymphatic system together form the cardiovascular system [17].

The heart cycle is a series of actions in a heartbeat. In general, the heart cycle consists of the synchronized contraction of both atria with a fraction of a second later, the synchronized contraction of each ventricle. The heart is made up of heart muscle cells that are interconnected with each other so that when one of them contracts, it leads to excitation of the neighboring cells. In the cardiac cycle, muscles are rested between beats, leading to breathe aerobically. There are two phases: phase 1: Systole is the expression for the contraction. This happens when the ventricles are in the contracting stage, causing the pumping of blood into the heart vessels with closure of the A-V valves and opening of the semilunar valves. Phase 2: Diastole is the expression for the relaxation. This happens when the ventricles are in a relaxing stage, causing the back-blood pressure to close the semilunar valves and open the A-V valves [18].

Any morphological changes or disorder of the heart rate can be indicative of cardiac arrhythmia which can be recorded and analyzed on ECG. The depolarization and repolarization of the sodium and potassium ions in the blood leads to the electrical wave. ECG can be used to gather information about the human heart such as heart position and chamber size, heart rate and rhythm, conduction disturbances, location and extent of ischemia, electrolyte disturbances, and effects of drugs on the heart as well as origin of impulses and propagation of impulses through the heart. ECG is digitally recorded for automatic processing and diagnosis. The goal of this paper is to detect HFD in early stages using ECG only and to see if HFD or other heart disorders are contented for each investigated interval.

A standard ECG is composed of 12 leads, a pair of electrodes that are placed on the body in certain positions and connected to an ECG recorder. The ECG is made of P wave, QRS complex and T wave with useful information contained in the amplitude and duration of the P-QRS-T wave in regards to the nature of the heart disease as shown in Fig.1 [19]. The P wave represents the depolarization and contraction of both right and left atria with low amplitude level voltage signal. P wave before a QRS signal represents normal sinus rhythm. Normal P wave is about 2-3 mv high in amplitude and is 0.06-0.12 seconds in duration. Absence of a P wave is suggestive of cardiac rhythm abnormality such as Atrial Fibrillation. P wave analysis may be difficult due to artifact on ECG. The QRS complex may vary in size based on gender and age. It is the largest voltage deflection at about 10-20 mV at an amplitude of 5-30 mv high with a duration of 0.06-0.10 seconds. The QRS complex is the time when the ventricles depolarize giving information about ventricular conduction issues such as bundle branch block. The T wave is repolarization of the ventricles. T wave abnormalities may represent ischemia or electrolyte abnormalities. The T wave is 0.5 mv in amplitude and duration of 0.1-0.25 seconds.

III. ELECTROCARDIOGRAM SIGNAL SEGMENTATION USING INFORMATION-THEORETIC

A. PROBLEM ILLUSTRATION

In this paper, ECG signal is segmented into five sections (P, Q, R, S, and T waves) based on time interval and peak value for each wave. It is also assumed that the three regions (P-QRS-T) are different in that they take changed probability amplitude functions for each positive amplitude and negative amplitude of the ECG waveform and that the time intervals borderline of the P-QRS-T waves inside the three segment areas are distributed and divided in an identical way. In this work, the detected ECG signal peak-values are presented as a spatial-random process $G(p)$ with time intervals index as presented in Fig.1.

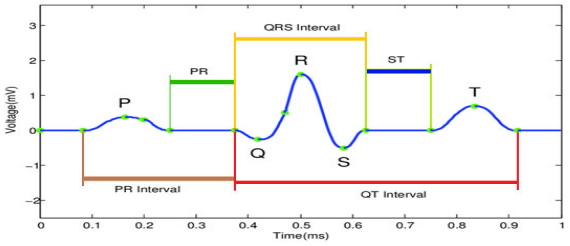

FIGURE 1. ECG waveform.

To differentiate between normal and abnormal ECG signal one should get the ECG amplitude for each part (P, Q, R, S, and T). In this technique, the ECG signal has been disintegrated/decomposed using the Discrete Wavelet Transform (DWT). The decomposition level for the DWT was selected so that the approximation coefficients of ISVM algorithm at this level corresponded to the time interval in ECG signal was located. To completely cancel the deviation from the baseline, the filtered ECG was then reconstructed by synthesizing the modified coefficients. The proposed technique $G(p)$ used with time intervals index to solve negative peaks (negative-amplitude) problems, the ECG is divided into sets of parts

each part has a specific amplitude according to time interval for each part (P, Q, R, S, and T).

Assume that $F(p)$ is the significant peak value of the ECG at the time interval p taken from the time interval d_1 if $p \in A_1$, and from d_2 if $p \in A_2$, $F(q)$ is the significant peak value of the ECG at the time interval q, taken from the time interval d_1 if $p \in A_1$, and from d_2 if $q \in A_2$, $F(r)$ is the significant peak value of the ECG at the time interval r, taken from the time interval d_1 if $p \in A_1$, and from d_2 if $q \in A_1$, $F(s)$ is the significant peak value of the ECG waveform at the time interval s, taken from the time interval d_1 if $p \in A_1$, and from d_2 if $p \in A_2$, *and* $F(t)$ is the significant peak value of the ECG waveform at the time interval t, taken from the time interval d_1 if $p \in A_1$, and from d_2 if $p \in A_2$ where A_1 and A_2, symbolise the two unidentified areas of the ECG signal, and p_1 and p_2 are unidentified correlating time intervals along ECG waveform. The correlating probability peak-values are unidentified, and the shape of these time intervals are not limited. So, the P, Q, R, S, and T peak-values of ECG waveform are defined as:

$$F(X)=\sum_{x=1}^{xn} F_p(x)-F_q(x)+F_r(x)-F_s(x)+F_t(x) \quad (1)$$

where $F_p(x) = \int_{x1}^{x2} pdx$, $F_q(x) = \int_{x2}^{x3} qdx$, $F_r(x) = \int_{x3}^{x4} rdx$, $F_s(x) = \int_{x4}^{x5} sdx$ *and* $F_x(x) = \int_{x5}^{x6} tdx$.

In this paper, the dual quadratic programming problem (QPP) is used to differentiate between each time interval of ECG signal according to peak values of P, Q, R, S, and T waves. The QPP is defined as a problem to optimize a quadradic objective function under given linear constraints [20]. QPP is to determine a vector $\bar{x} = (x_1, \ldots, x_n)^T$ that solves the problem: $\min f(x)$ subject to $g_i(x) \leq 0, i = 1, \ldots, m$ and $h_j(x) = 0, j = 1, \ldots, l$, $x \in R^n$, where x is a vector of design variables, $f(x) : R^n \rightarrow R$ is called the objective function. The dual problem of QPP is formatted by using the Lagrange dual function of the quadratic objective function which is $\phi : R^n \times R^p \times R^l \rightarrow R$ defined by:

$\phi(x, \mu, \lambda) = f(x) + \sum_{i=1}^{p} \mu_i g_i(x) + \sum_{j=1}^{l} \lambda_j h_j(x) = f(x) + \mu^t g(x) + \lambda^t h(x)$. So, the Lagrange dual function $\theta : R^p \times R^l \rightarrow R$ is defined as:

$$\begin{aligned} \theta(\mu, \lambda) &= \inf_{x \in R^n} \phi(x, \mu, \lambda) \\ &= \inf_{x \in R^n} (f(x) + \mu^t g(x) + \lambda^t h(x)). \end{aligned} \quad (2)$$

where $\mu_i \& \lambda_j$ are called dual variables. μ_i is nonnegative and associated with inequality constraints $g_i(x) \leq 0$ and λ_j is unrestricted in sign and associated with equalities constraints $h_j(x) = 0$. The form of dual problem to problem (1) is defined as follow:

$$\begin{aligned} &\max \ \theta(\mu, \lambda) \\ &\text{subject to } \mu \geq 0 \end{aligned} \quad (3)$$

where $(\mu, \lambda) \inf \left\{ \begin{matrix} f(x) + \sum_{i=1}^{m} \mu_i g_i(x) \\ + \sum_{j=1}^{l} \lambda_j h_j(x) \end{matrix} \middle| x \in R^n \right\}$.

The optimal solutions set (Oss) of the dual problem are defined as:

$$Oss = \{\bar{\mu} \geq 0, \bar{\lambda} | \theta(\bar{\mu}, \bar{\lambda}) = \max_{\mu \geq 0} \theta(\mu, \lambda) \quad (4)$$

B. ECG SIGNAL PRE-PROCESSING USING NONPARAMETRIC ALGORITHM

In this paper, the nonparametric algorithm distributes the ECG waveform into unknown areas with different time intervals. It divides ECG waveform into n-regions ($D_1, D_2, \ldots, D_n$ denote the real unknown areas) with each area having an unknown time interval $x_1, x_2, \ldots, x_n$ respectively. The peak values of ECG signal at P, Q, R, S, and T waveforms, denoted by y, is drawn from the X_i if P, Q, R, S *and* $T \in D_i$. The peak values in the ECG waveform within each area are correlated with the probability time interval which are not already known. The curve estimation of the ECG waveform segmentation moves a set of curves $\left\{\vec{S}_1, \vec{S}_2, \ldots, \vec{S}_m\right\}$ (equivalently, a level-set functions $\{q_1, \ldots, q_m\}$) to divide the ECG domain. Each curve S_i divides the domain of the ECG into seven areas: the P, Q, R, S, and T waves and the area inside and outside of the curve [21], [22]. The ECG domain for each cycle is divided into 2^m areas which are represented by the signs of the set of level functions in that region. The peak values of ECG signal submitted as redundant zones procedure $Y(y)$ with time interval index is a collection of multiple peak different elements as shown in Fig.2.

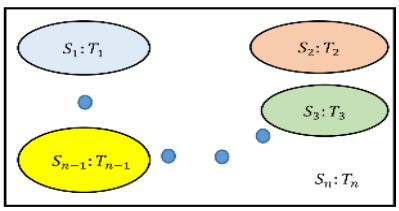

FIGURE 2. The ECG waveform is divided into $S_1, \ldots, S_n$ with Time interval $T_1, \ldots, T_n$.

The n-area ECG time intervals are used in the curve development approach to draw a curve $\vec{S}$ touching the boundary between D_i and D_j, the internal area of the curve D_+ intersects at D_i and the external area intersects at D_j, as shown in Fig.3. $\vec{S}$ is function of t, time component that can be ignored, $\vec{S} = \vec{S}(t)$. This splitting of the ECG waveform produces a binary label $L_{\vec{S}}(y) : D \rightarrow \{L_+, L_-\}$, which is a component of the ECG waveform D to a set of two labels $\{L_+, L_-\}$. $L_{\vec{S}}(x) = L_+$ if $x \in D_i$ and $L_{\vec{S}}(x) = L_-$ if $x \in D_j$.

Given the areas divided by the curves $S \left\{\vec{S}_i\right\}_{i=1}^{m}$, one-can denote every peak in the ECG waveform by x label $L_S(x)$. Let a label $L_S : D \rightarrow \left\{L_{s(i+)}, L_{s(i-)}\right\}$.

$$L_S(x) = L_{s(i+)} \ if \ y \in D_{s(i+)}, \quad 1 \leq i \leq 2^{m-1} \quad (5)$$

$$L_S(x) = L_{s(i-)} \ if \ y \in D_{s(i-)}, \quad 2^{m-1} + 1 \leq i \leq 2^m \quad (6)$$

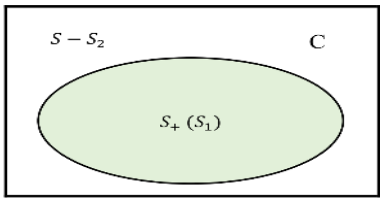

FIGURE 3. The basic determination of the curve $(\vec{c})$.

where $s(i+)$ is the ith element in the set-level $\{L_{++\cdots+}, \ldots, L_{+-\cdots-}\}$ and $s(i-)$ is the ith element in the set-level $\{L_{-+\cdots+}, \ldots, L_{--\cdots-}\}$.

A peak x in D is randomly selected such that x is a regularly distributed random position in the ECG domain and the label $L_{\vec{S}}(x)$ is a random variable that depends on the curve $\vec{S}$ [21], [23]. The values $L_{s(i+)}$ and $L_{s(i-)}$ are taken with probability $\left|D_{s(i+)}\right| / |D|$ and $\left|D_{s(i-)}\right| / |D|$, respectively where $\left|D_{s(i+)}\right|$ denotes the area of the section$D_{s(i+)}$. Furthermore, the peak-value y is a random variable that depends on the true sections D_i, and has the following time interval [24]–[26]:

$$Q_y(v) = \sum_{i=1}^{n} P_r\left(x \in D_i\right)_{Q_{Y(y)|y\in D_i}(v)} = \sum_{i=1}^{n} \frac{|D_i|}{|D|} Q_i(v) \quad (7)$$

where v is an argument for the time intervals and $P_{Y(y)}$ is a combination of Q_i due to the randomness of the peak position x. The improbability of peak l position being in D_i and the improbability of the most-significant amplitude given the peak position. The label $L_{\vec{S}}(x)$ includes some information about the former improbability, namely x, being in D_i or D_j.

Subsequently, the more precise the label $L_{\vec{S}}(x)$ can determine if $x \in D_i$, the less improbability $D(x)$ has more details about $Y(y)$ then the label will have. Use of the mutual data $d\left(Y(y) : L_{\vec{S}}(x)\right)$ as a criterion of segmentation [21], [23]. The mutual data is:

$$\begin{aligned} &d\left(Y(y) : L_{\vec{S}}(x)\right) \\ &= k\left(Y(y)\right) - k\left(Y(y)|L_{\vec{S}}(x)\right) \\ &= k\left(Y(y)\right) - \sum_{i=1}^{2^m} P_r\left(L_{\vec{S}}(x) = L_{s(i+)}\right) k\left(Y(y)|L_{\vec{S}}(x) = L_{s(i+)}\right) \\ &\quad - \sum_{i=2^{m-1}+1}^{2^m} P_r\left(L_{\vec{S}}(x) = L_{s(i-)}\right) k\left(Y(y)|L_{\vec{S}}(x) = L_{s(i-)}\right) \end{aligned}$$

where $k(W)$ is the differential entropy of a random variable W with support s is defined by $k(W) = -\int_s Q_W(v) \log Q_W(v) dv$ [27], [28]. The three entropies in equation (6) are functions of $Q_{Y(y)}$, $Q_{Y(y)|L_{\vec{S}}(x)=L_{s(i+)}}$ and $Q_{F(Y)|L_{\vec{S}}(Y)=L_{s(i-)}}$ respectively. The two restricted distributions are given as follows:

$$\begin{aligned} &Q_{Y(y)|L_{\vec{S}}(x)=L_{s(i+)}}(v) \\ &= \sum_{i=1}^{n} P_r\left(x \in D_i|L_{\vec{S}}(x) = L_{s(i+)}\right)_{Q_{Y(y)|x\in D_i, L_{\vec{S}}(x)=L_{s(i+)}}(v)} \\ &= \sum\nolimits_{i=1}^{n} \frac{\left|D_{s(i+)} \cap D_i\right|}{\left|D_{s(i+)}\right|} Q_i(v) \end{aligned} \quad (8)$$

$$\begin{aligned} &Q_{Y(y)|L_{\vec{S}}(x)=L_{s(i-)}}(v) \\ &= \sum_{i=1}^{n} P_r\left(x \in D_i|L_{\vec{S}}(x) = L_{s(i-)}\right)_{Q_{Y(y)|x\in D_i, L_{\vec{S}}(x)=L_{s(i-)}}(v)} \\ &= \sum\nolimits_{i=1}^{n} \frac{\left|D_{s(i-)} \cap D_i\right|}{\left|D_{s(i-)}\right|} Q_i(v) \end{aligned} \quad (9)$$

Each dependent entropy measures the heterogeneity degree in each zone/time interval determined by the curve $\vec{S}$. The more identical the segmented areas, the higher the mutual peaks and the uncertain entropies, which is an appropriate property for segmentation [27], [29]. The shared peak is maximized if and only if it is the true segmentation, if, $D_{s(i+)} = D_i, D_{s(i-)} = D_j$ (or, equivalently $D_{s(i-)} = D_i, D_{s(i+)} = D_j$).

Practically, one is unable to calculate the mutual data $d\left(Y(y) : L_{\vec{S}}(x)\right)$ because the previous calculations involve the sections D_i and D_j, and peak-time intervals Q_i and Q_j which were unidentified to us [21], [25], [26]. In energy functionality, mutual data should be weighted by the peak and time interval ECG domain to represent the over-all mutual information among the ECG waves for each peak value and time interval since $d\left(Y(y); L_{\vec{S}}(x)\right)$ matches to the contribution of a one peak to the overall information. The resultant energy is given by

$$E\left(\vec{S}\right) = -|D|\,\hat{d}\left(Y(y); L_{\vec{S}}(x)\right) + a \oint_{\vec{S}} ds \quad (10)$$

where $\oint_{\vec{S}} ds$ is the total curve length and a is a scalar factor.

This section includes the derivation of the curve estimation formula to minimize the energy function. First, how to approximate the conditional entropy conditions using the nonparametric estimations technique [30]. Reference [31] is presented. Second, how to determine gradient flow for $E\left(\vec{S}\right)$.

The equation (8) is used to compute the differential entropies. Subsequently $\hat{k}(D(x))$ in equation (8) is independent of the length of the curve, Thus:

$$\begin{aligned} &\hat{k}\left(Y(y)|L_{\vec{S}}(x) = L_{s(i+)}\right) \\ &= -\frac{1}{\left|D_{s(i+)}\right|} \int_{D_{s(i+)}} \log \hat{Q}_{s(i+)}\left(Y(y)\right) dy \\ &= -\frac{1}{\left|D_{s(i+)}\right|} \int_{D_{s(i+)}} \log\left(\frac{1}{\left|D_{s(i+)}\right|} \int_{D_{s(i+)}} V(Y(y) - Y(\hat{y})) d\hat{y}\right) \end{aligned} \quad (11)$$

It is found that $k\left(F(Y)|L_{\vec{S}}(x) = L_{s(i+)}\right)$ contains the predictable value of the approach of $Q_{s(i+)} \triangleq Q_{F(Y)|L_{\vec{S}}(x)=L_{s(i+)}}$, and utilize the kernel

$$V(v) = \left(1/\sqrt{2\pi b^2}\right) e^{-v^2/2b^2} \quad (12)$$

where b is a scalar factor. Correspondingly, Thus,

$$\begin{aligned} &\hat{k}\left(Y(y)|L_{\vec{S}}(x) = L_{s(i-)}\right) \\ &= -\frac{1}{\left|D_{s(i-)}\right|} \int_{D_{s(i-)}} \log \hat{Q}_{s(i+)}\left(Y(y)\right) dy \end{aligned}$$

$$= -\frac{1}{\left|D_{s(i-)}\right|}\int_{D_{s(i-)_-}} \times \log\left(\frac{1}{\left|D_{s(i-)}\right|}\int_{D_{s(i-)}} V(Y(y)-Y(\hat{y}))d\hat{y}\right)dy \quad (13)$$

Consequently, equations (12) and (14) have nested area integrals. It is assumed that an over-all nested section integral of the form

$$E\left(\vec{S}\,(t)\right) = \int_D f\left(\varepsilon\,(y,t)\right)dQ \quad (14)$$

where $\varepsilon\,(y,t) = \int\limits_D g(y,\hat{y})d\hat{y}$ and g independent on $\vec{S}$ [18], [20], D is the range within the curve $\vec{S}$. So, the integral of the area decreases further rapidly and known by

$$\frac{\partial\vec{S}}{\partial t} = -\left[f\left(\varepsilon\left(\vec{S}\right)\right) + \int_N f'\left(\varepsilon\,(y)\right)g(y,\vec{S})dy\right]\vec{n} \quad (15)$$

where $\vec{n}$ is the unit vector outwardly. Not that the $f\,(\varepsilon\,(y,t))$ in equation (14) depends on the curve length $\vec{S}$.

The nonparametric assessments of the shared data in the form of nested area, as in equations (12) and (14), it is easy to approximate the overall gradient flow for $E\left(\vec{S}\right)$ (energy functional) of equation (11). The energy functional $E\left(\vec{S}\right)$ can be written as:

$$\left(\vec{S}\right) = -\left|D\right|\hat{k}\,(Y(y)) + E_-\left(\vec{S}\right) + E_+\left(\vec{S}\right) + a\oint_{\vec{S}} ds \quad (16)$$

where the components $E_-\left(\vec{S}\right) = \sum\limits_{i=2^{m-1}+1}^{2^m} E_{s(i-)}\left(\vec{S}\right)$; $E_+\left(\vec{S}\right) = \sum\limits_{i=1}^{2^{m-1}} E_{s(i+)}\left(\vec{S}\right)$ are given by

$$E_{s(i+)}\left(\vec{S}\right) = \left|D\right|P_r\left(L_{\vec{S}}(x) = L_{s(i+)}\right)k\left(Y(y)|L_{\vec{S}}\,(y) = L_{s(i+)}\right) = -\int\limits_{D_{s(i+)}} \log\left(\frac{1}{\left|D_{s(i+)}\right|}\int\limits_{D_{s(i+)}} V\left(Y\,(y) - Y(\hat{y})\right)d\hat{y}\right)dy \quad (17)$$

Since in $1/\left|D_{s(i+)}\right|$ depends on the curve, E_+ are segmented into two integrals. The gradient flow for E_+ is computed as:

$$E_{s(i+)} = E^1_{s(i+)} + E^2_{s(i+)} \quad (18)$$

where

$$E^1_{s(i+)} = -\int\limits_{D_{s(i+)}} \log\left|D_{s(i+)}\right|dy = -\left|D_{s(i+)}\right|\log\left|D_{s(i+)}\right|$$

and

$$E^2_{s(i+)} = \int\limits_{D_{s(i+)}} \log\left(\int\limits_{D_{s(i+)}} V\left(Y(y) - Y(\vec{S})\right)d\hat{y}\right)dy.$$

The gradient flow for $E^2_{s(i+)}$ is $\nabla_{\vec{S}}E^2_{s(i+)}$, given by:

$$\nabla_{\vec{S}}E^1_{s(i+)} = -\nabla_{\vec{S}}\left|D_{s(i+)}\right|\log\left|D_{s(i+)}\right| - \nabla_{\vec{S}}\left|D_{s(i+)}\right| = \left(1+\log\left|D_{s(i+)}\right|\right)\vec{n} \quad (19)$$

$$\nabla_{\vec{S}}E^1_+ = \sum_{i=1}^{2^{m-1}}\left(1+\log\left|D_{s(i+)}\right|\right)\vec{n}.$$

$$\nabla_{\vec{S}}E_+ = \nabla_{\vec{S}}E^1_+ + \nabla_{\vec{S}}E^2_+ \quad (20)$$

where

$$\nabla_{\vec{S}}E_+ = \sum\nolimits_{i=1}^{2^{m-1}}\left[-1+\log Q_{s(i+)}\left(Y\left(\vec{S}\right)\right) + \frac{1}{\left|D_{s(i+)}\right|}\int_{D_{s(i+)}}\frac{V\left(Y\,(y) - Y\left(\vec{S}\right)\right)}{\hat{Q}_{s(i+)}\,(Y\,(y))}dy\right]\vec{n}$$

$$\nabla_{\vec{S}}E_- = \sum\nolimits_{i=2^{m-1}+1}^{2^m}\left[1-\log Q_{s(i-)}\left(Y(\vec{S})\right) - \frac{1}{\left|D_{s(i-)}\right|}\int_{D_{s(i-)}}\frac{V(Y(y)-Y(\vec{S}))}{\hat{Q}_{s(i-)}(Y(y))}dy\right]\vec{n}.$$

Then the gradient flow for $E\left(\vec{S}\right)$ of (18) is obtainable as follows:

$$\frac{\partial\vec{S}}{\partial t} = \sum_{i=1}^{2^{m-1}}\left[\log Q_{s(i+)}\left(Y(\vec{S})\right) + \frac{1}{\left|D_{s(i+)}\right|}\int_{D_{s(i+)}}\frac{V(Y(y)-Y(\vec{S}))}{\hat{Q}_{s(i+)}Y(y))}dy\right]\vec{n} - \sum_{i=2^{m-1}+1}^{2^m}\left[\log Q_{s(i-)}\left(F(\vec{S})\right) + \frac{1}{\left|D_{s(i-)}\right|}\int_{D_{s(i-)}}\frac{V(Y(y)-Y(\vec{S}))}{\hat{Q}_{s(i-)}(Y(y))}dy\right]\vec{n} - ak\vec{n} \quad (21)$$

where $-ak\vec{n}$ is the gradient flow for the length of the curve and k is the curve curvature [21], [23], [26].

The calculations take at each iteration $O((nQmberof\ peaks)^2)$. The calculation of the first term calculation along the curvature takes $O\left(N(|D_+| + |D_-|)\right)$ time, where N is the number of peaks on the curve (the narrow-band size). While the second term evaluations calculate and store $\hat{Q}_+\,(Y(y))\,\forall x \in D_+$. The time of this evaluations takes $O(|D_+|^2)$ and integrated with the stored values of $\hat{Q}_+(Y\,(y))$. This integral calculation along the curve takes $O\left(|D_+|^2\right)$ time [21], [26] so it takes $O\,(d\,|D_+|)$ time to calculate the integration at all points of the curve. Thus, the difficulty of a direct calculation of the gradient flow is of all peaks $O(N\,(|D_+| + |D_-|) + |D_+|^2 + |D_-|^2 + N\,(|D_+| + |D_-|)$ at every step.

To compute time interval of ECG waveform according to peak-values by Gauss transformation in the form $Q\,(y) = (1/M)\sum_{i=1}^{M} V(y-y_i)$ at N different peaks in $O\,(c(N+M))$ time instead of $O\,(NM)$ time to decrease computational complexity, where M peaks information, c is the number of accuracy which produces the required precision of the

approach (9), (11). c is considered less than 10 in most cases. Using a randomly selected subset of D_+ is sufficient, rather than using the total peak-amplitudes in D_+ to evaluate $\hat{Q}_+$. So, choosing M peaks from D_+ to estimate $\hat{Q}_+$ and select another M peaks from D_-, the computational procedure is $O(c(N+M+M+c\,(M+M)+c\,(N+M)+c\,(M+M)+c\,(N+M)$ by using the fast Gauss transform in every iteration.

The time of integration calculation of the second and the third part in the equation (18), (20) is $O\,(c(N+M))$ time by the fast Gauss transform. Due to the size of the narrow band, N will be chosen as a linear function of N. If the length of the curve expression is replaced as in the active geodesic peak-borders, the estimation equation (18) will be div $((g(y,y)\nabla Q/|\nabla Q|)\,|\nabla Q|$ substituted from the curvature of the curve flow, where q is the suitable set of level function [32]. The first part of the gradient flow in the equation (18) is a log-LA which compares the conventions that the peak-values of the observed ECG-waveform $Y(\vec{S})$ at a given peak on the active border belongs to the back-ground area D_- or the foreground area D_+ based upon the present evaluations of the distributions Q_+ and Q_-. By using log-LA term, the peak on the contour is integrated to either the region or the zone such that the updated areas are identical.

IV. THE IDENTIFICATION HYBRID APPROACH

This paper focuses on the identification of the main common type of heart disease from ECG waveform. A new technique is introduced to identify the HFD from the patient's ECG with a more accurate diagnosis than the current methods. The introduced algorithm is applied to ECG to detect HFD using ISVM based on DO. In this method, m level-set functions are used to segment up to $2^{\mathrm{m}}\pm$ peak-values according to their time intervals and the equation of the resulting evolution curve is proving to be an actual generalization of the dual-SVM sensitivity area competition as shown in Fig 4.

A. THE DUALITY OF SUPPORT VECTOR MACHINE

The five-sections ECG waveform identification problem to a n-area technique is presented, where $S_1,\ldots,S_n$ represent the real unidentified peak-values for each P, Q, R, S, and T in the ECG waveform, represented by a $y_i f\,(x_i)$ is acquired from the time interval index $x_1,\ldots,x_n$. As known the SVM is defined as min $\|f(x)\|_k^2+\sum_{i=1}^{l} c_i\varepsilon_i$ Subject to

$$y_i f\,(x_i)\geq 1-\varepsilon_i,\quad i=1,\ldots,l\;\forall\varepsilon_i\geq 0 \tag{22}$$

The Lagrange dual function of problem (23) is the function $\phi: R^n\times R^p\times R^l\to R$ defined by [30]:

$\phi\,(x,\mu,\lambda)=\|f(x)\|_k^2+\sum_{i=1}^{l} c_i\varepsilon_i-\sum_{i=1}^{l}\mu_i\,(y_i f\,(x_i)-1+\varepsilon_i)-\sum_{i=1}^{l} a_i\varepsilon_i=\|f(x)\|_k^2+\sum_{i=1}^{l}(c_i-a_i-\mu_i)\,\varepsilon_i-\sum_{i=1}^{l}\mu_i\,(y_i f\,(x_i)-1)$.

The Lagrange dual function $\theta: R^p\times R^l\to R$ as:

$$\begin{aligned}\theta\,(\mu,\lambda)&=\phi\,(x,\mu,\lambda)\\&=\left(f(x)+\mu^t\,((yf(x)-1+\varepsilon))+a^t\varepsilon\right)\end{aligned} \tag{23}$$

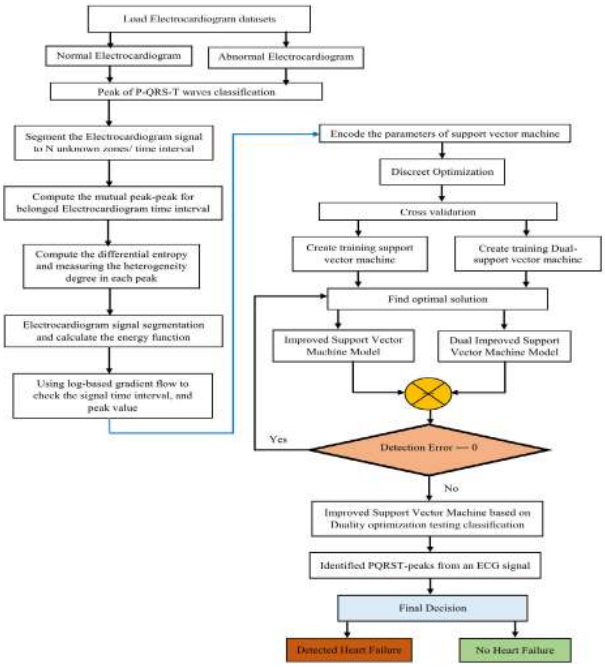

FIGURE 4. Algorithm of ISVM based on DO method.

where μ&a are called dual variables. μ is associated with the inequality constraints $y_i f\,(x_i)\geq 1-\varepsilon_i$ and is nonnegative while a is associated with the inequality constraint ε_i and is nonnegative.

$$\begin{aligned}&\max\;\theta\,(\mu,\lambda)\\&\text{Subject to}\;\mu,\quad a\geq 0\end{aligned} \tag{24}$$

In the duality technique, there are two theorems: the first one is weak duality (WD) theorem and the second one is strong duality (SD) theorem. In WD theorem, let x be a feasible solution to problem (23) that is $x\in X, g(x)\leq 0, h(x)=0$. Also (μ,λ) be a feasible solution to problem (18) with $\mu\geq 0$, then

$$\theta(\mu,\lambda)\leq\|f(x)\|_k^2+\sum_{i=1}^{l} c_i\varepsilon_i \tag{25}$$

In this case, we assume that the optimum objective function values of the original and dual problem are equal according to constraints qualification and convexity assumptions.

In SD theorem, let X be a nonempty convex set in R^n. Let $f: R^n\to R, g: R^n\to R^m$, and $h: R^n\to R^l$ be affine. Suppose that the following constraint qualification holds true [33], [34]. There exist $\bar{x}\in X$ such that $g\,(\bar{x})<0$, $h\,(\bar{x})=0$, and $0\in$ int $h(X)$, where $h(X)=\{h(x)|x\in X\}$.

$$\begin{aligned}&\inf\{f(x)|x\in X, g(x)\leq 0, h(x)=0\}\\&\qquad=\sup\{\theta\,(\mu,\lambda)|\mu\geq 0\}\end{aligned} \tag{26}$$

Furthermore, if $\inf\{f(x)|x\in X, g(x)\leq 0, h(x)=0\}$ is finite then $\sup\{\theta\,(\mu,\lambda)|\mu\geq 0\}$ is achieved at $(\bar{\mu},\bar{\lambda})$ with $\bar{\mu}\geq 0$. If inf is achieved at $\bar{x}$ then$\bar{\mu}^t g\,(\bar{x})=0$.

B. THE DUALITY TECHNIQUE OPTIMIZATION

The primal problem (23) defines two Lagrange functions known as the lower Lagrange function $\phi_*(x,\mu,\lambda) = f(x) + \mu^t G(x) + \lambda^t H(x)$ and the upper Lagrange function $\phi^*(x,\mu,\lambda) = f(x) + \mu^t g(x) + \lambda^t h(x)$. A solution $(\bar{x},\bar{\mu},\bar{\lambda})$ is called a saddle point of Lagrange function if $\bar{x} \in X$, $\bar{\mu} \geq 0$ and

$$\phi(\bar{x},\mu,\lambda) \leq \phi(\bar{x},\bar{\mu},\bar{\lambda}) \leq \phi(x,\bar{\mu},\bar{\lambda}) \tag{27}$$

For all $x \in X$ and all (μ,λ) with $\mu \geq 0$.

Therefore, $\bar{x}$ minimizes ϕ over X when (μ,λ) is fixed at$(\bar{\mu},\bar{\lambda})$, and that $(\bar{\mu},\bar{\lambda})$ maximizes ϕ over all(μ,λ) with $\bar{\mu} \geq 0$ when x is fixed at $\bar{x}$.

Now, to find Saddle point optimality and absence of a duality gap for the upper Lagrange function (ULF), we assume that a solution is $(\bar{x},\bar{\mu},\bar{\lambda})$ with $\bar{x} \in X_*$ and $\bar{\mu} \geq 0$ for the ULF $\phi(x,\mu,\lambda) = f(x) + \mu^t g(x) + \lambda^t h(x)$. If and only if $(\bar{\mu},\bar{\lambda}) = \phi(\bar{x},\bar{\mu},\bar{\lambda}) = \min\{\phi(x,\bar{\mu},\bar{\lambda}) | x \in Xg(\bar{x}) \leq 0, h(\bar{x}) = 0, \bar{\mu}^t g(\bar{x}) = 0$. Moreover, $(\bar{x},\bar{\mu},\bar{\lambda})$ it is a saddle point if and only if $\bar{x}$ and $(\bar{\mu},\bar{\lambda})$ are respectively optimal solutions to the primal problem (23) on the lower approximation set and the upper approximation dual problem (25) with no duality gap that is with $f(\bar{x}) = \theta(\bar{\mu},\bar{\lambda})$ [30], [35].

Now one can calculate the relationship between the saddle point criteria and Karush-Kuhn- Tucker (KKT) conditions as follows. It is assumed the item X is a set $(X = \{x \in X | g(x) \leq 0, h(x) = 0\})$ and consider problem (23) to minimize $f(x)$ subject to $x \in X$. Suppose that $\bar{x} \in X$ satisfies the KKT conditions, that is, there exist $\bar{\mu} \geq 0$ and $\bar{\lambda}$ such that

$$\begin{aligned} \nabla f(\bar{x}) + \nabla g(\bar{x})^t \bar{\mu} + \nabla h(\bar{x})^t \bar{\lambda} = 0 \\ \bar{\mu}^t g(x) = 0 \end{aligned} \tag{28}$$

The proposed approach assumes that f and g_i for $i \in I$ are convex at $\bar{x}$, where $I = \{i | g_i(\bar{x}) = 0\}$. Further, suppose that if $\bar{\lambda}_i \neq 0$, then h_i is affine. Then $(\bar{x},\bar{\mu},\bar{\lambda})$ is a saddle point for upper Lagrange function $\phi(x,\mu,\lambda) = f(x) + \mu^t g(x) + \lambda^t h(x)$. Conversely, suppose that $(\bar{x},\bar{\mu},\bar{\lambda})$ with $\bar{x} \in \text{int } X$ and $\bar{\mu} \geq 0$ is a saddle point solution. Then $\bar{x}$ is a feasible to problem (23), and furthermore, $(\bar{x},\bar{\mu},\bar{\lambda})$ satisfies the KKT conditions specified by [34].

To calculate the standard deviation and mean value of the proposed approach, let $p, p_2, \ldots, p_s$ a set of discrete random variables were the average of the random variable p describes where the most significant peak in ECG signal is centered (36):

$$\mu = \frac{p_1 + p_2 + \cdots + p_N}{s} = \frac{1}{s}\sum_{i=1}^{s} p_i \tag{29}$$

Since the proposed algorithm is applied to five groups, each group contains 35 recordings of ECG signals generated from 1200 different subjects taken from real patient's data with HFD taken from PhysioNet database [37]. Therefore, one mean is calculated as:

$$\mu_x = \sum_{i=1}^{s} p_i f_i(p) \tag{30}$$

where S is the number of peaks that belong to time interval. Now the variance can be used to represent an important measure of variability of the variable in the segmented peak as follow:

$$\sigma_x^2 = \sum_{i=1}^{S} (p - \mu_p)^2 f_i(p) \tag{31}$$

V. HFD IDENTIFICATION PERFORMANCE

To assess the performance studied and tested ECG signal identification techniques, the comparison is calculated as a reference using the following parameters between the identified ECG signal obtained from all the methods studied and the segmented ECG signal occasioned from the proposed method.

A. ECG DICE SIMILARITY COEFFICIENT (DC)

The ECG waveform is made up of numerous peaks like any other digital signal. The chief task is to determine which peaks signify HFD. The Dice similarity coefficient provides a mathematical solution for this difference. Fig. 2 presents five areas of the ECG waveform of the same construction D and X, where D is the real unknown amplitude $(d_1, d_2, \ldots, d_n)$ inside C_1 and X is the unknown time interval $(x_1, x_2, \ldots, x_n)$ inside C_2. In this illustration, the five-peaks of interest have different circular shapes, time intervals and locations. When D and X are the reference mask area that the space between the two peaks as the integration mask area section of the ECG signal manually the segment of the ECG waveform is indicated by a result of an algorithm, DC is measured as follows:

$$DC = \frac{2(\mathrm{D} \cap \mathrm{X})}{D + X} \tag{32}$$

It is an association between the two neighbor peaks of overlap of the two time intervals or positions which is dispersed into two areas D and X. So, $0 \leq DC \leq 1$, where 1 is the full consent and 0 does not mean overlap at all.

B. QUALITY OF PEAK SEGMENTATION USING PSNR

Peak signal-to-noise ratio (PSNR) is a measure metric of the efficiency of ECG signal segmentation. The *PSNR*is an expression for the relationship between the maximum probable value of an ECG signal and the power of distorting noise that affects the quality of its representation. Because ECG waveforms have very wide dynamic range on the time frequency plane, the PSNR is usually expressed in terms of the logarithmic decibel scale.

$$PSNR = 10\log\left(\frac{(MU)^2}{MSE(D,\mathrm{X})}\right) \tag{33}$$

where $MSE(D,\mathrm{X}) = \frac{1}{m}\sum_{i=1}^{m}(U_i - \bar{U}_i)^2$, U_i is the vector of $\pm$ peak-value of the P, Q, R, S, and T waves being detected with $\bar{U}_i$ is a vector of m time intervals on all peaks generated randomly. MU is the most significant peak-value for each part of the ECG signal domain.

C. HAUSSDORFF DISTANCE

The distance between the two dual-peaks of a metric space will be measured using the Haussdorff (HD) metric. The distance *HD* is the minimum distance from any peak on the other side of a segment. This means that part of the amplitude of one of the desired peaks of each P, Q, R, S, and T in the ECG waveform defines the lowermost distance on the other side of the wanted peak and the greater most distance *HD* of these values.

$$HD = \max\left\{\sup_{u\in D}\inf_{y\in X} L(u,y), \sup_{y\in X}\inf_{u\in D} L(u,y)\right\} \quad (34)$$

where $L(u, y) = |u - y|$.

VI. EXPERIMENTAL RESULTS

In this paper, the presented technique was applied to many different datasets to show its ability to detect HFD using ECG signal. The presented results were obtained by using an improved support vector machine algorithm on five groups of real data taken from Physio-Bank. The data base was generated from 1200 different ECG signals taken from different patients with different types of heart diseases especially heart failure disease. The ECG database contains 38 recordings with heart failure disease with each record having a duration of 30 minutes [37]. This HFD database contains greater than 89,000 pulses that are categorized independently with one of five possible categories. In all illustrations, the regularization constraint in the equations (4) and/or (22) and/or (29) was instinctively chosen based on a qualitative manuscript assessment of segmented ECG signals. In situations where earlier records are attainable about heart failure disease in patient's ECG waveform, it may be adept to acquire an appropriate regularized distribution according to the classified features of HFD (Peak's and time interval's) combined through the signal/noise ratio (SNR) of the segmented ECG-peak. To demonstrate the proposed technique, the ISVM-DO algorithm is applied to many ECG signals used before in several preceding papers. Fig. 5 presents the ECG signal with P, Q, R, S, and T peaks for any patient with HFD. Fig.5 (a) presents the normal ECG signal. In a normal ECG waveform, the heart rate at a constant sinus rhythm between 60 and 100 beats/minute. It is found that all significant peak-values and time intervals of this record fall within the normal range. In this signal, the p-wave is mostly smooth with duration equal to 0.11 sec, the duration of PR-wave is 0.16 sec, the QRS complex has duration 0.10 sec, and the peak-peak value equal to 2.51mV with the duration of QT-wave is 0.40 sec. Fig.5 (b) presents the sample of patient's ECG waveform with heart failure disease. Fig.5 (c) illustrates the patient's ECG waveform (noisy) without pre-processing. The main purpose of the pre-processing step is to increase the SNR of the patient's ECG waveform to highlight the QRS complex, P, R, and T waves by suppressing the interference of power lines and high-frequency noise from the patient's ECG waveform. Fig.5 (d) presents the patient's ECG waveform after noise reduction to be clear. Fig.6 (a) presents the ECG

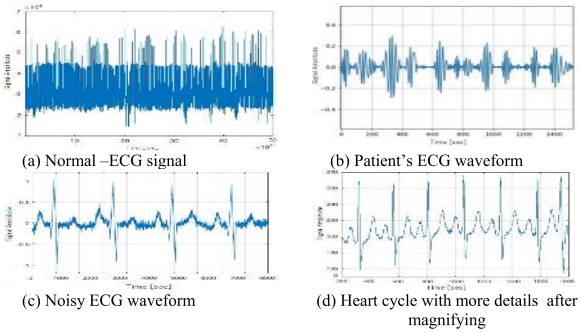

(a) Normal –ECG signal (b) Patient's ECG waveform
(c) Noisy ECG waveform (d) Heart cycle with more details after magnifying

FIGURE 5. ECG signal with P, Q, R, S, and T peaks of any person.

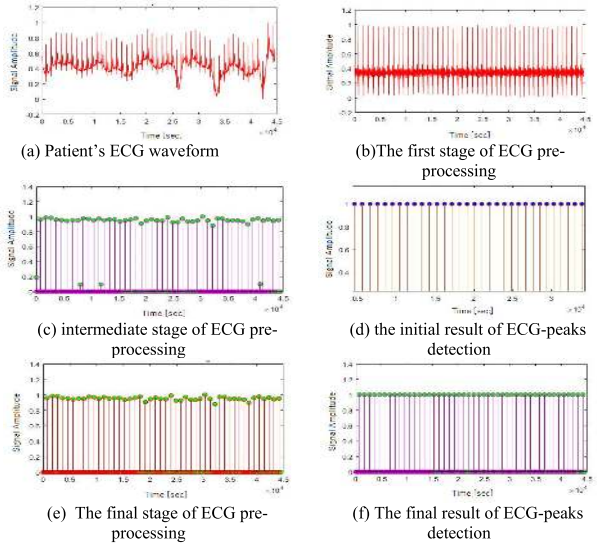

(a) Patient's ECG waveform (b)The first stage of ECG pre-processing
(c) intermediate stage of ECG pre-processing (d) the initial result of ECG-peaks detection
(e) The final stage of ECG pre-processing (f) The final result of ECG-peaks detection

FIGURE 6. The first stage results of the ISVM-DO on the ECG signal.

signal taken from a sick person with a heart rate equal to 115 beats/minute. The duration of p-wave is 0.17 se, PR-wave is 0.24 sec, and the QRS complex has a duration 0.19 sec and the peak-peak value equal to 3.15mV. Fig.6 (b) shows the patient's ECG signal after the first stage of ECG pre-processing. This signal contains P, Q, R, S and T waves with different time intervals. The peak value for each part in the ECG waveform is a single peak with a specific duration. It was found that all peaks have comparable variance and mean, so even for a cardiologist, it is challenging to detect the HFD from this waveform. So as to improve the processed ECG waveform, we have used the low pass filter (LPF) and high pass filter (HPF) in pre-processing step as shown in Fig.6 (c) and (e). Fig.6 (f) shows the results constructed by the proposed algorithm for the final pre-processing stage where the ECG-peak in the processed waveform is detected. To evaluate the log-based in equation (12) and present the significance of using it from the use of the three terms in the equation (22), the amplitudes acquired during the process of curve evaluation were collected and introduced histograms of them in Fig. 7, to show the significance in the estimation process. Fig. 7(a) shows the histograms acquired by using the first term of equation (22) of the ECG amplitudes. It is recognized that the values of the first terms are frequently

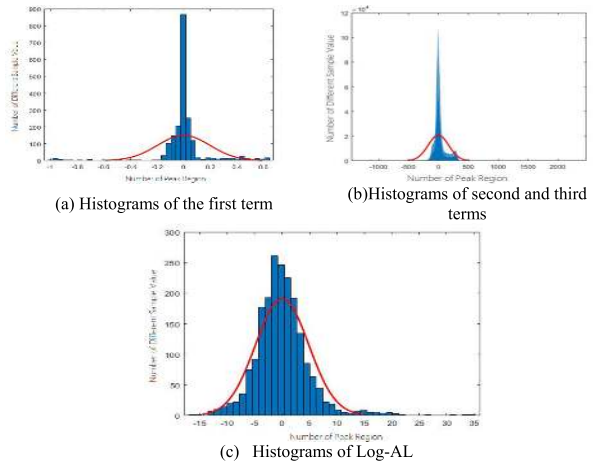

(a) Histograms of the first term

(b)Histograms of second and third terms

(c) Histograms of Log-AL

FIGURE 7. Histogram outcomes of the proposed algorithm terms for the peaks in a ECG waveform.

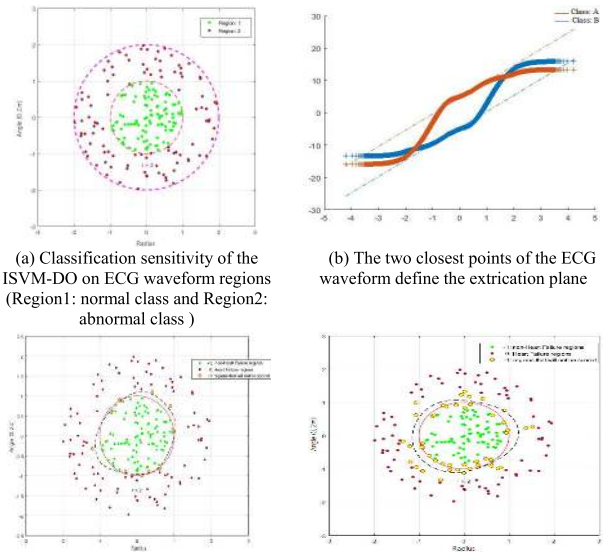

(a) Classification sensitivity of the ISVM-DO on ECG waveform regions (Region1: normal class and Region2: abnormal class)

(b) The two closest points of the ECG waveform define the extrication plane

(c) The intermediate HFD classification

(d) The final HFD classification

FIGURE 8. The classification results of the ISVM-DO on the ECG signal.

close to two and within a range between −1.0 and 2.7. Fig.7 (b) shows the results done by the second and third terms in equation (22). It is found that both terms have a limited value and their differences have a limited range between −3.0 and 3.0. Finally, Fig.7 (c) shows the results of log-based in equation (22). One can identify that mainly the first terms of equation (22) have greater magnitude compared to the second and third terms in equation (12) and their difference. Therefore, it is used as the leading provider to the peak estimation.

This section illustrates how to detect the HFD in ECG signals according to peak-peak amplitudes and time intervals as one zone in model construction using improved support vector machine (ISVM) based on duality optimization (DO) technique. In this algorithm, HFD has been detected in ECG waveforms by identifying the hyper-optimal plane that divides HFD-datasets to maximize the margin between them. It is found that, all vectors that are close to the hyperplane are the support vectors.

The easiest method to boundary two categories (HFD or No heart failure disease (NHFD)) is with two circles having N-dimensional hyperplane as shown in Fig. 8 (a). Therefore, the final decision should be restricted as much as achievable in relation to the ECG database of the two classifications as shown in Fig. 8 (b). To get the final decision as two categories (HFD or NHFD), the ISVM based on DO is used to represent the ECG database to another space in which a hyperplane can be used to perform the separation. In the proposed technique, a class of points are generated in the circle of the two-dimensional unit and another class of points are generated in the second circle with the radius ($r = 2$) as shown in Fig. 8 (c). An improved support vector machine (ISVM) classifier is generated based on duality optimization (DO) technique to perform an exact classification, which means that no learning point is incorrect. This method can distinguish different peak-peak values correlated to time interval in ECG signals with several amplitudes and durations of the P-QRS-T waves. Fig. 8 (d) shows the final results of HFD classification using ISVM-DO. In this method, the gradient flow is used to identify ± peak-value and time interval borderline according to their location in ECG signal and the position both inside and outside. A low frequency filter with DPF is used to remove a noise from ECG signals for the final multi-scale procedure, which assures these ECG signal improvements. Thus, the Gaussian conditional field is constructed to acquire the net ECG signal under the noisy input. Finally, the segmented ECG signal containing P, Q, R, S, and T waves is acquired. The identification results were categorized into three types of classification: region (+1) with HFD, region (0) without HFD and region (−1) with other heart disease. The ISVM-DO rejects any unspecified peak and has higher complete identification, which makes it the preferred algorithm for this task of identifying the HFD from ECG recordings. The ISVM's success is because of the ability of the classifier to build an optimum and decide complicated decision boundary for the learning ECG database. Due to that the ECG database cannot be classified non-linearly, it is the most complex problem in this type of datasets. So the most current classification methods cannot solve this problem completely, but the proposed algorithm can do by invoking the pre-processing stage repeatedly based on duality optimization and comparing the processing results with the last decision taken before the moments when the classifier was unable to make a dependable decision. In Fig. 8 (d) the nearest peak points in the reduced convex shape are represented by a circle. The ISVM-DO formulation supposes that the optimal hyperplane sprats the two parallel margin planes according to duality optimization method. In a sense, the hyperplane goes to the class where it is more reliable. This characteristic was also observed in the proposed ISVM-DO formulations to detect peak-peak values correlated to their time intervals in ECG signal based, which differ from all current methods

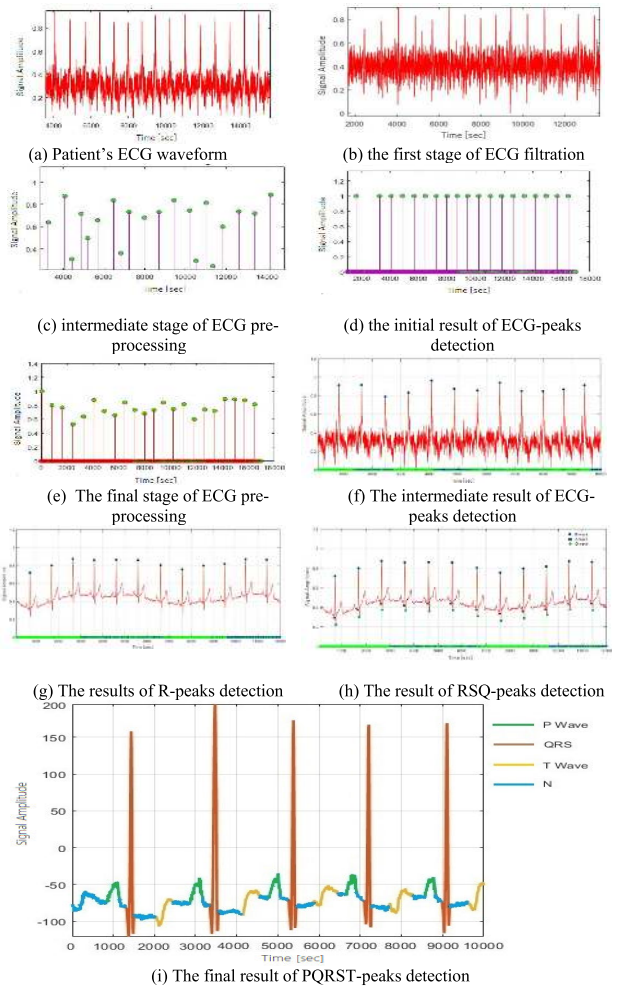

FIGURE 9. The final results of the ISVM-DO on the ECG signal.

such as SVM toolset based on LIBSVM, SVM based on RBF, SVM based on SMO and OLS, and ANN based on LVQ and MLP formulations. It uses duality optimization according to different threshold margins for each peak-class instead of one variable for each. Therefore, the peak-value and time interval changes in ECG signal can be identified as splitting and merging and singularities on the curve such as sharp corners. Fig. 9 shows the ECG signal taken from a sick person with the heart rate equal to 108 beats/minute, the duration of p-wave is 0.18 sec, PR-wave is 0.26 sec, the QRS complex has duration 0.19 sec and the peak-peak value equal to 3.18mV. Patients with HFD have an irregular heartbeat. Fig.9 (a) shows the patient's ECG signal with a large range of abnormalities and other clinical pathological entities. Fig.9 (b) shows the patient's ECG signal after the first stage of ECG pre-processing. This signal indicates that the amplitude of P, Q, R, S and T waves with different time intervals attended with noise such as Gaussian white noise etc. To improve the patient's ECG signal, the band pass filter (BPF) that was used as a low pass filter (LPF) in the first stage of pre-processing step and then a high pass filter (HPF) was used in the second stage as shown in Fig.9 (c) and (e). The pre-processing stage requires a high speed of filtration process to identify location of poles. In this stage, the BPF used has the frequency band of approximately 10 to 18 Hz. Fig.9 (d) and (f) show the intermediate result of ECG-peaks detection. Integration of the ECG signal is done and it has been through the differential entropy of a random variable with support vector machine according to the BPF time interval. So, the correlating probability of all peak-values in ECG waveform are identified according to the shape of their time intervals. In addition, the gradient flow function has been combined with the duality optimization method for computing the $\pm$ peak-value and time interval borderline of P, Q, R, S and T waves in the processed ECG signal. In most of the patient's ECG records, the QRS-waves have a large amplitude and long duration especially in patient's recorded with HFD. So, the cardiologist cannot only use the R-wave to detect abnormalities in ECG signals. Therefore, in this method, the gradient of the peak of R-waves are considered as an appropriate method to identify the QRS complexes in the patient's ECG signal. Fig. 9 (i) shows the final results obtained by the ISVM-DO formula finding the two nearest points in the desired area, including peak-peak value and time intervals and, as an experiential, selecting the threshold midway between the adjacent peak points. Therefore, by identifying the P-QRS-T amplitude and duration waves in the patient's ECG signal, HFD can be detected and compared with the normal range of the P-QRS-T waves in normal ECG signal.

VII. COMPARATIVE ANALYSIS AND CASE STUDY

The proposed technique is applied to 38 recordings of real data of ECG signals with HFD taken from PhysioNet database. A Five-section (P, Q, R, S, and T) ECG signal segmentation problem is considered for each record. It is also considered that the three areas (P, QRS, and T) are different in that they yield different probability peak-peak and time interval borderline of all waves in the patient's ECG. It is found that the three sections in the processed ECG signal are distributed and separated in an identical way. The ISVM-DO can identify all peak values of P, Q, R, S, and T waves in the ECG waveform for any patient with HFD. Consequently, the significant morphological properties in the processed ECG are extracted using this algorithm. The identification results for each group are tabulated in tables 1, 2, 3, 4 and 5. The tables illustrate the comparative results of the P, Q, R, S, T, QRS complex and HFD detection using ISVM based on duality technique. Each table shows one group only which contains 38 recordings taken from patients with and without HFD with each record has duration of 30 minutes. The proposed algorithm has been applied to P, Q, R, S, T, and QRS complex of raw ECG and processed ECG to find the detection percentage of HFD. The HFD detection percentage were obtained for each normal and abnormal ECG waveform. To find the detection error of the proposed algorithm, the identification result for each P, Q, R, S, T, and QRS complex is represented as positive detection (amplitude of the

TABLE 1. The result of HFD identification using ISVM Technique for group #1.

Peak-Name		Detection Percentage			
		Normal ECG Signal		Abnormal ECG Signal	
		pstive	*nagtive*	*pstive*	*nagtive*
Raw ECG	P	68.9	31.1	48	52
	Q	73.4	26.6	52.5	47.5
	R	84.5	15.5	63.6	36.4
	S	34.5	65.5	13.6	86.4
	T	34.2	65.8	13.3	86.7
	QRS-	67.5	32.5	46.6	53.4
	HFD	---	---	24.4	75.6
Identification %		58.3	41.7	37.4	62.6
Processed ECG	P	96.9	3.1	97.6	2.4
	Q	93.8	6.2	90.5	9.5
	R	99.2	0.8	97.1	2.9
	S	90.4	9.6	93.8	6.2
	T	94.5	5.5	90.9	9.1
	QRS-	98.3	1.7	98	2
	HFD	---	---	98.6	1.4
Identification %		96	4	95.2	4.8

TABLE 2. The result of HFD identification using ISVM Technique for group #2.

Peak-Name		Detection Percentage			
		Normal ECG Signal		Abnormal ECG Signal	
		pstive	*nagtive*	*pstive*	*nagtive*
Raw ECG	P	78.8	21.2	86.8	13.2
	Q	83.3	16.7	63.4	36.6
	R	94.4	5.6	89.3	10.7
	S	44.4	55.6	70.1	29.9
	T	44.1	55.9	84.4	15.6
	QRS-	77.4	22.6	65.2	34.8
	HFD	---	---	84.8	15.2
Identification %		68.2	31.8	77.8	22.3
Processed ECG	P	96.8	3.2	91.9	8.1
	Q	96.3	3.7	95.6	4.4
	R	99.2	0.8	97.5	2.5
	S	90.9	9.1	92.3	7.7
	T	98.3	1.7	96.6	3.4
	QRS-	99.1	0.9	97.4	2.6
	HFD	---	---	97.1	2.9
Identification %		97	3	95.5	4.5

TABLE 3. The result of HFD identification using ISVM Technique for group #3.

Peak-Name		Detection Percentage			
		Normal ECG Signal		Abnormal ECG Signal	
		pstive	*nagtive*	*pstive*	*nagtive*
Raw ECG	P	79.1	20.9	70.4	29.6
	Q	83.6	16.4	77	23
	R	94.7	5.3	72.9	27.1
	S	44.7	55.3	73.6	26.4
	T	44.4	55.6	78	22
	QRS-	77.7	22.3	61	39
	HFD	---	---	78.1	21.9
Identification %		68.5	31.5	73	27
Processed ECG	P	92.5	7.5	93.5	6.5
	Q	99.1	0.9	89.1	10.9
	R	98.5	1.5	99.5	0.5
	S	95.7	4.3	95.7	4.3
	T	90.1	9.9	94.1	5.9
	QRS-	96.3	3.7	90.9	9.1
	HFD	---	---	98.9	1.1
Identification %		96	4	94.5	5.5

peak-peak is detected) and negative detection (amplitude of the peak-peak is not detected). In those tables, It was found that the average percentage of HFD detection of group #1 approximately 58.03% to 62.16 % for raw ECG and 93.23% to 96.21%. For the processed ECG, group #2

TABLE 4. The result of HFD identification using ISVM Technique for group #4.

Peak-Name		Detection Percentage			
		Normal ECG Signal		Abnormal ECG Signal	
		pstive	*nagtive*	*pstive*	*nagtive*
Raw ECG	P	58.7	41.3	64.3	35.7
	Q	63.2	36.8	68.8	31.2
	R	74.3	25.7	79.9	20.1
	S	64.3	35.7	69.9	30.1
	T	64	36	69.6	30.4
	QRS-	57.3	42.7	62.9	37.1
	HFD	---	---	80.7	19.3
Identification %		65.3	34.7	70.9	29.1
Processed ECG	P	92.3	7.7	89.9	10.1
	Q	98.9	1.1	94.4	5.6
	R	94.8	5.2	95.5	4.5
	S	95.5	4.5	97.2	2.8
	T	99.9	0.1	95.8	4.2
	QRS-	94.7	5.3	98.1	1.9
	HFD	---	---	93.3	6.7
Identification %		96.3	3.7	94.9	5.1

TABLE 5. The result of HFD identification using ISVM Technique for group #5.

Peak-Name		Detection Percentage			
		Normal ECG Signal		Abnormal ECG Signal	
		pstive	*nagtive*	*pstive*	*nagtive*
Raw ECG	P	74.3	25.7	84.3	15.7
	Q	78.8	21.2	90.9	9.1
	R	89.9	10.1	90.3	9.7
	S	39.9	60.1	87.5	12.5
	T	39.6	60.4	91.9	8.1
	QRS-	72.9	27.1	98.1	1.9
	HFD	---	---	91.5	8.5
Identification %		63.7	36.3	90.6	9.4
Processed ECG	P	92.1	7.9	90.3	9.7
	Q	94.7	5.3	97.9	2.1
	R	98.1	1.9	96.3	3.7
	S	95.3	4.7	94.5	5.5
	T	95.7	4.3	95.9	4.1
	QRS-	97.8	2.2	92.1	7.9
	HFD	---	---	95.5	4.5
Identification %		96	4	94.6	5.4

approximately 68.08% to 77.64% for raw ECG and 95.60% to 97.21%. For processed ECG, group #3 approximately 68.50% to 73.44% for raw ECG and 94.80% to 96.71%. For processed ECG, group #4 approximately 65.29% to 73.14% for raw ECG and 94.98% to 96.51%. For processed ECG, group #5 approximately 63.98% to 73.64% for raw ECG and 94.68% to 96.01% for processed ECG. Total percent of peak detection of P, Q, R, S, T, and QRS complex waves for all groups is illustrated in table 6. This table is calculated using tables1, 2, 3, 4 and 5. As seen in table 6, the average results of HFD detection for all groups that were acquired from the proposed approach are approximately 63.7% to 69.9% for raw ECG, and 94.9% to 96.2% for processed ECG. For all groups, the average result is 94.97%.

VIII. PERFORMANCE EVALUATION AND CROSS-VALIDATION

The performance metrics for the proposed method (ISVM-DO) are computed and compared with four classification methods, including Chen'S LIBSVM [10], Vadicherla'S SVM-SMO [11], Lewicke's MLP NN [12], and Ghumbre's SVM- OLS [13]. To evaluate the HF identification performance of the proposed method, we implemented the

TABLE 6. The overall results of HFD identification using ISVM for all groups.

	Peak-Name	Detection Percentage			
		Normal ECG Signal		Abnormal ECG Signal	
		pstive	*nagtive*	*pstive*	*nagtive*
Raw ECG	Group#1	58.3	41.7	37.4	62.6
	Group#2	68.2	31.8	77.8	22.3
	Group#3	68.5	31.5	73	27
	Group#4	65.3	34.7	70.9	29.1
	Group#5	63.7	36.3	90.6	9.4
Identification %		64.8	35.2	69.9	30.1
Processed ECG	Group#1	96	4	95.2	4.8
	Group#2	97	3	95.5	4.5
	Group#3	96	4	94.5	5.5
	Group#4	96.3	3.7	94.9	5.1
	Group#5	96	4	94.6	5.4
Overall Average		96.2	3.7	94.9	5.1

TABLE 7. The result of the cross-validation results on raw-ECG datasets.

HFD-Identification Methods	Recall	Precision	Specificity	Accuracy	Composite Measure (CM)
Chen'S LIBSVM	0.528	0.792	0.875	0.675	0.662
Vadicherla's SVM-SMO	0.54	0.891	0.951	0.662	0.612
Lewicke's MLP NN	0.301	0.781	0.932	0.428	0.421
Ghumbre's SVM- OLS	0.721	0.724	0.752	0.752	0.762
ISVM-DO	0.874	0.681	0.701	0.793	0.801

TABLE 8. The result of the cross-validation results on processed ECG datasets.

HFD-Identification Methods	*Recall*	*Precision*	*Specificity*	*Accuracy*	*Composite Measure (CM)*
Chen'S LIBSVM	0.548	0.812	0.895	0.695	0.682
Vadicherla's SVM-SMO	0.560	0.911	0.971	0.682	0.632
Lewicke's MLP NN	0.321	0.801	0.952	0.448	0.441
Ghumbre's SVM- OLS	0.741	0.744	0.772	0.772	0.782
ISVM-DO	0.894	0.661	0.681	0.813	0.821

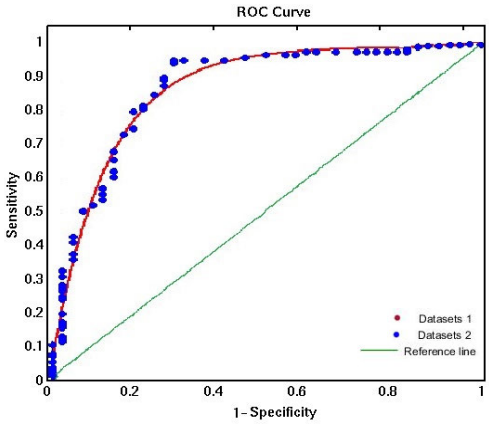

FIGURE 10. Fig. 10 shows the ROC curves of the proposed method (ISVM-DO) on Raw-ECG dataset and processed-ECG dataset.

following generally used measures: Precision $= P_T/(P_T + P_F)$, Sensitivity $= P_T/(N_T + P_F)$, Specificity $= N_T/(N_T + P_F)$, Accuracy $= (P_T + N_T)/(P_T + P_F + N_T + N_F)$, and Composite Measure (CM) score $= 2((Precision \times Recall)/(Precision + Recall))$, where P_T is true positives, P_F is the false positives, N_T is the true negatives, and N_F is the false negatives. To train the predictor of the proposed algorithm, several cross-validation tests and random tests were applied to 125 samples from the training dataset. This procedure was repeated 15 times to acquire the average result. As seen in Table 7 for all groups (Raw ECG), the proposed method (ISVM-DO) has the greatest recall of 0.894 and CM score of 0.821 compared to the other four methods. Table 8 shows the results of cross-validation on the processed ECG dataset. As seen in Table 8 for all groups, the ISVM-DO has distinguish–performance; with the highest recall of 0.91 and CM score 0.85. Moreover, the accuracy and specificity of the proposed technique are also competitive. Fig. 10 shows the ROC curves of the proposed method for all groups including Raw ECG dataset and processed ECG dataset. As seen in Fig.10, the total area under the curves is 0.863 for Raw-ECG and 0.842 processed-ECG datasets.

Table 9 shows the result of the mean and standard deviation of the ISVM-DO technique for all groups. The mean value and standard deviation are obtained using equations (30-32). As seen in table 9 for all groups, the average value of the mean and the standard deviation for the proposed technique are $\mu = 0.58067354$ and $\sigma = 0.13767174$ for patient's ECG of all groups, and $\mu = 0.56665863$ and $\sigma = 0.13764045$ for processed ECG. In Table 9, the mean and standard deviation of presented approach is very sensitive to the peak-peak identification in patient's ECG waveform and the detection of HFD is very sensitive. Table 10, shows the comparison between the proposed method and some other methods (Chen'S LIBSVM, Vadicherla'S SVM-SMO, Lewicke's MLP NN, and Ghumbre's SVM- OLS) based on *DM*, *PSNR* and *HS* which are shown in equations (33-35). The comparison is applied to 38 recordings of real data of ECG signals taken from patients with and without HFD which are grouped into five groups. We start the comparison on the known five (P, Q, R, S, and T) peaks in ECG waveform. The DM, PSNR, HS and exaction time for each group are calculated. The averages of DM, PSNR, HS and exaction time are summarized at the end of table 10. The key performance metrics of HFD identification using the preceding studied methods are recorded for each of the same three datasets presented above as sample results. The results presented in table 10 enforce the previously concluded results. The proposed technique detected HFD in patient's ECG signal successfully using improved support vector machine based on duality technique. In this technique, a nonparametric statistical method is used for ECG

TABLE 9. The result of the mean and standard deviation of the ISVM-DO Technique for all groups.

ECG-Waveform/group			Group number				
			Group #1	Group #2	Group #3	Group #4	Group #5
Normal ECG	*Input ECG signal*	μ	0.404833913	0.327512430	0.403993040	0.327515893	0.405457268
		σ	0.2922298313	0.3064847283	0.0291771863	0.0301788983	0.2928378623
	Processed ECG signal	μ	0.327515142	0.406165678	0.328354056	0.406706046	0.330497056
		σ	0.3067451773	0.0291961503	0.0300945483	0.2930112183	0.3064753693
Abnormal ECG	*Input ECG signal*	μ	0.611644948	0.534323465	0.610804075	0.534326928	0.612268303
		σ	0.0292127593	0.0301068353	0.2934335523	0.0291883893	0.3064171753
	Processed ECG signal	μ	0.534326177	0.612976713	0.535165091	0.613517081	0.537308091
		σ	0.0300940373	0.2937791543	0.3054482523	0.0292979503	0.0295828503

TABLE 10. The comparison results based on DM, PSNR and HS for five HFD-identification methods.

No. of group	HFD-Identification Methods	DM	PSNR	HS	Execution time
Group #1	Chen'S LIBSVM	0.8957	20.5605	16.2605	3.718734
	Vadicherla'S SVM-SMO	0.9019	22.8505	10.5705	2.598504
	Lewicke's MLP NN	0.4108	11.6605	150.7105	8.781804
	Ghumbre's SVM- OLS	0.9026	24.5705	12.1505	3.372594
	ISVM-DO	0.9557	24.8305	7.74054	2.089434
Group #2	Chen'S LIBSVM	0.8717	21.0805	15.6805	3.057171
	Vadicherla'S SVM-SMO	0.8107	23.3005	9.98054	2.500504
	Lewicke's MLP NN	0.3827	10.4405	150.8095	8.157171
	Ghumbre's SVM- OLS	0.8137	23.2205	11.9205	3.307171
	ISVM-DO	0.9407	23.4705	7.63054	2.093837
Group #3	Chen'S LIBSVM	0.8607	21.6205	12.3205	3.217171
	Vadicherla'S SVM-SMO	0.8707	22.0005	8.9805	3.037171
	Lewicke's MLP NN	0.3407	10.2605	151.7305	8.080504
	Ghumbre's SVM- OLS	0.8807	22.1305	9.9205	3.483837
	ISVM-DO	0.9609	21.9005	8.9805	1.897171
Group #4	Chen'S LIBSVM	0.8307	23.2505	8.7305	3.263837
	Vadicherla'S SVM-SMO	0.9007	23.4105	7.3205	2.973837
	Lewicke's MLP NN	0.3107	9.78050	154.5605	8.023837
	Ghumbre's SVM- OLS	0.8907	24.9405	5.9205	4.013837
	ISVM-DO	0.9507	23.1705	7.9905	2.067171
Group #5	Chen'S LIBSVM	0.8207	19.8805	18.7211	3.207171
	Vadicherla'S SVM-SMO	0.9407	26.6105	5.0405	2.970504
	Lewicke's MLP NN	0.3207	9.99050	153.0805	7.933837
	Ghumbre's SVM- OLS	0.8807	22.6305	9.9205	3.423837
	ISVM-DO	0.9707	26.1805	5.1605	2.057171
Overall Average results	Chen'S LIBSVM	0.8957	20.5605	16.2611	3.718734
	Vadicherla'S SVM-SMO	0.9017	22.8505	10.5171	2.598504
	Lewicke's MLP NN	0.4107	11.6605	150.7105	8.781804
	Ghumbre's SVM- OLS	0.9007	24.5705	12.1051	3.372594
	ISVM-DO	0.9601	24.8305	7.7405	2.089434

TABLE 11. The overall comparative results of HFD identification using different methods.

HFD/ Group	Identification Techniques				
	Chen'S LIBSVM	Vadicherla'S SVM-SMO	Lewicke's MLP NN	Ghumbre's SVM- OLS	ISVM-DO
Group #1	70.43%	70.74%	83.43%	80.43%	95.21%
Group #2	53.24%	81.54%	79.76%	79.76%	95.53%
Group #3	70.97%	82.65%	83.22%	79.22%	94.50%
Group #4	68.23%	75.78%	72.54%	78.54%	94.95%
Group #5	64.67%	64.28%	85.62%	78.62%	94.67%
Overall Average	65.51%	75.00%	80.91%	79.31%	94.97%

signal segmentation. This technique focuses on a multivariate analysis of a set of physiological parameters that were applied to P-QRS-T wave, for HFD detection based on information theory, parameter optimization and nonparametric estimation techniques. The high calculation time is mostly because the technique requires the calculation of local data for each point of the interface developed in each step. Also, Lewicke's MLP NN and Ghumbre's SVM-OLS have good values in HS but the proposed algorithm has the best value in HS, PSNR and DM among all other methods as seen in table 10. At the end of this comparison, the proposed approach has better values than other methods depending on the execution time, HS, PSNR and DM. Table 11 shows the overall comparative results of the detection of HFD using different methods

TABLE 12. A list of Major symbols used in this paper.

Abbreviation	Explanation	Abbreviation	Explanation
HFD	Heart Failure Disease	$G(p)$	Spatial-Random Process
ECG	Electrocardiogram	**QPP**	Dual Quadratic Programming Problem
SVM	Support Vector Machine	μ, λ *and* **a**	Dual Variables
SMO	Sequential Minimum Optimization	$g_i(x)$	Inequality Constraints
ANN	Artificial Neural Network	$h_j(x)$	Equalities Constraints
LVQ	Learning Vector Quantization	Oss	Optimal Solutions Set
MLP	Multilayer Perceptron	S_l	Curve Estimation
RBF	Radial Basis Function	$L_{\bar{S}}(x)$	Random Variable
OLS	Orthogonal Least Square	b	Scalar Factor
MLPNN	Multilayer Perceptron Neural Network	**WD**	Weak Duality
LVQNN	Learning Vector Quantization Neural Network	**SD**	Strong Duality
OLS	Orthogonal Square Minimum Algorithm	**ULF**	Upper Lagrange Function
ISVM	Improved Support Vector Machine	**KKT**	Karush-Kuhn- Tucker
DO	Duality Optimization	**DC**	*Dice Coefficient*
$F(p)$	Significant Peak Value of the ECG At The Time interval p	**PSNR**	Peak Signal-To-Noise Ratio
$F(r)$	Significant Peak Value of the ECG At The Time interval r	**HD**	*Hausdorff Distance*

(Chen'S LIBSVM, Vadicherla'S SVM-SMO, Lewicke's MLP NN, and Ghumbre's SVM- OLS). In experimental results, after applying the proposed technique on patient's ECG signal that taken from five groups, it was found that the average percentage of HFD detection is 94.97%. The average percentage of HFD detection of Chen'S LIBSVM is 65.51%, Vadicherla'S SVM-SMO is 75.0%, Lewicke's MLP NN is 80.91% and Ghumbre's SVM- OLS is 79.31%. At the end of this comparison, the identification of HFD in patient's ECG signal using the proposed ISVM algorithm based on duality technique is generating robust identification for heart failure disease compared to the other detection methods. Experiments show that the proposed approach produces good results with increasing reliability and accuracy of prediction, and identification of heart failure disease in the early stages using the proposed algorithm from an ECG signal only. Table 12 is summarizing the major symbols used in this paper for easy reference.

IX. CONCLUSION

A new approach is presented in this paper to detect heart failure disease (HFD) by using improved support vector machine (ISVM) based on duality optimization (DO) technique. The proposed technique differentiates between normal and abnormal ECG signals based on heart rate duration of PQRST waves leading to predicting and diagnosing the HF from an ECG signal only. The SVM and the dual SVM are used to improve performance of the algorithm. In this algorithm, amplitude and time interval are used as one zone in model formation. The SVM and the dual SVM are very effective because duality gives a different yet complementary view of the ECG signal. The proposed idea is based on using the non-parametric approach to train ISVM and its dual to get two models of SVM. The two models are used to detect HFD in the ECG signal which contains P, Q, R, S, and T waves and compare their peak-peak values. If the result of the comparison is zero, the ISVM output is obtained. Otherwise, both outputs are used to feed each other. In this method, three probabilities are considered: the first one indicates region (+1) with HFD, the second indicates region (0) without HFD and the third indicates region (−1) with other heart disease (abnormal ECG wave but does not contains HFD). The noise is eliminated by using digital pass filter (DPF) in pre-processing stage. The output results obtained from the proposed approach on test cases show better results than the results other methods yield. The proposed algorithm saves the diagnostic time and costs and improves treatment process accuracy. The obtained results indicate that the proposed technique produces good results, is more efficient and increases the accuracy of HFD detection with an acceptable accuracy of 94.97% compared to the other algorithms to which the article refers, particularly in patients with multiple diseases not initially identified as HFD.

In our future work, we will examine on the one hand the more useful features of chronic disease classification in biomedical signals, and we will try to develop more prediction methods based on advanced machine learning techniques. Many signal processing applications could benefit from this approach, where the signal peak-peak is correlated to time interval using duality optimization method in chronic diseases classification such as Obstructive Sleep Apnea classification using electroencephalogram, airflow and Oxygen saturation signals could be used to ensure reliable classification.

REFERENCES

[1] W. B. Kannel and A. J. Belanger, "Epidemiology of heart failure," *Amer. Heart J.*, vol. 121, no. 3, pp. 951–957, 1991.
[2] P. H. Thakur, B. E. Koop, Q. An, and K. R. Maile, "Diastolic endocardial accelerations for heart failure monitoring," U.S. Patent 15 675 279, Feb. 15, 2018.
[3] S. M. Day, P. M. Elliott, and G. Limongelli, "Clinical and molecular aspects of cardiomyopathies: On the road from gene to therapy," *Heart Failure Clinics*, vol. 14, no. 2, pp. 1551–7136, 2018.
[4] A. L. Phillips, M. Y. Qureshi, B. W. Eidem, and F. Cetta, "Lambl's excrescences in children: Improved detection via transthoracic echocardiography," *Congenital Heart Disease*, vol. 13, no. 2, pp. 251–253, 2018.
[5] R. T. Müller, *Trauma and the Struggle to Open Up: From Avoidance to Recovery and Growth*. New York, NY, USA: WW Norton & Company, 2018.
[6] S. Latreche, N. Methia, M. Djouhri, and S. Benkhedda, "2D stain, speckle tracking: A sensitive factor of assessment of the effectiveness for chronic heart failure treatment," *Arch. Cardiovascular Diseases Supplements*, vol. 10, no. 1, p. 48, 2018.

[7] S. Achenbach, T. Giesler, D. Ropers, S. Ulzheimer, H. Derlien, C. Schulte, and E. Wenkel, "Detection of coronary artery stenoses by contrast-enhanced, retrospectively electrocardiographically-gated, multislice spiral computed tomography," *Circulation*, vol. 103, no. 21, pp. 2535–2538, 2001.

[8] A. P. Maggioni, R. Latini, P. E. Carson, S. N. Singh, S. Barlera, R. Glazer, S. Masson, E. Cerè, G. Tognoni, and J. N. Cohn, "Valsartan reduces the incidence of atrial fibrillation in patients with heart failure: Results from the Valsartan heart failure trial (Val-HeFT)," *Amer. Heart J.*, vol. 149, no. 3, pp. 548–557, 2005.

[9] D. Dickstein, K. A. Cohen-Solal, G. Filippatos, J. J. V. McMurray, P. Ponikowski, P. A. Poole-Wilson, and A. Stromberg, "ESC guidelines for the diagnosis and treatment of acute and chronic heart failure," *Eur. J. Heart Failure*, vol. 10, no. 10, pp. 933–989, 2008.

[10] C.-J. Chen, Y.-T. Lo, J.-L. Huang, T.-W. Pai, M.-H. Liu, and C.-H. Wang, "Feature analysis on heart failure classes and associated medications," in *Proc. IEEE Int. Conf. Syst., Man, Cybern. (SMC)*, Oct. 2016, pp. 1382–1387.

[11] D. Vadicherla and S. Sonawane, "Classification of heart disease using SVM And ANN," *Int. J. Res. Comput. Commun. Technol.*, vol. 2, no. 9, pp. 693–701, 2013.

[12] A. Lewicke, E. Sazonov, M. J. Corwin, M. Neuman, and S. Schuckers, "Sleep versus wake classification from heart rate variability using computational intelligence: Consideration of rejection in classification models," *IEEE Trans. Biomed. Eng.*, vol. 55, no. 1, pp. 108–118, Jan. 2008.

[13] S. Ghumbre, C. Patil, and A. Ghatol, "Heart disease diagnosis using support vector machine," in *Proc. Int. Conf. Comput. Sci. Inf. Technol. (ICCSIT)*, Pattaya, Thailand, 2011, pp. 1–5.

[14] M. Hammad, A. Maher, K. Wang, F. Jiang, and M. Amrani, "Detection of abnormal heart conditions based on characteristics of ECG signals," *Measurement*, vol. 125, pp. 634–644, Sep. 2018.

[15] M. Amrani, M. Hammad, F. Jiang, K. Wang, and A. Amrani, "Very deep feature extraction and fusion for arrhythmias detection," *Neural Comput. Appl.*, vol. 30, no. 7, pp. 2047–2057, Oct. 2018.

[16] M. Hammad, S. Zhang, and K. Wang, "A novel two-dimensional ECG feature extraction and classification algorithm based on convolution neural network for human authentication," *Future Gener. Comput. Syst.*, vol. 101, pp. 180–196, Dec. 2019.

[17] *Understanding the Circulatory System*. Accessed: Jan. 14, 2019. [Online]. Available: http://www.aspenpharma.eu/services/thrombosis-knowledge-center/circulatory-system/

[18] R. F. Rushmer, "Structure and function of the cardiovascular system," in *Handbook of Research Methods in Cardiovascular Behavioral Medicine*. Boston, MA, USA: Springer, 1989, pp. 5–22.

[19] A. Atkielski, *Schematic Diagram of Normal Sinus Rhythm for a Human Heart as Seen on ECG*. Accessed: Jan. 14, 2019. [Online]. Available: http://en.wikipedia.org/wiki/Image:SinusRhythmLabels.svg

[20] M. S. Bazaraa, H. D. Sherali, and C. M. Shetty, *Nonlinear Programming: Theory and Algorithms*. Hoboken, NJ, USA: Wiley, 2013.

[21] G. G. N. Geweid, M. A. Elsisy, O. S. Faragallah, and R. Fazel-Razai, "Efficient tumor detection in medical images using pixel intensity estimation based on nonparametric approach," *Expert Syst. Appl.*, vol. 120, no. 1, pp. 139–154, 2019.

[22] J. L. Sanz-Gonzalez, F. Alvarez-Vaquero, and J. E. Gonzalez-Garcia, "Permutation test algorithms for nonparametric radar detection," in *Proc. IET Int. Conf. Radar Syst.*, Oct. 2007, pp. 1–5.

[23] P. R. White, "Non-parametric techniques for the estimation of spatial spectra in non-stationary environments," *IET Radar, Sonar Navigat.*, vol. 1, no. 3, pp. 184–190, Jun. 2007.

[24] C. Li, C.-Y. Kao, J. C. Gore, and Z. Ding, "Minimization of region-scalable fitting energy for image segmentation," *IEEE Trans. Image Process.*, vol. 17, no. 10, pp. 1940–1949, Oct. 2008.

[25] O. Ronneberger, P. Fischer, and T. Brox, "U-Net: Convolutional networks for biomedical image segmentation," in *Proc. Int. Conf. Med. Image Comput. Comput.-Assist. Intervent.* Cham, Switzerland: Springer, Oct. 2015, pp. 234–241.

[26] Y. Wang and C. He, "Adaptive level set evolution starting with a constant function," *Appl. Math. Model.*, vol. 36, no. 7, pp. 3217–3228, 2012.

[27] M. R. Zare, A. Mueen, M. Awedh, and W. C. Seng, "Automatic classification of medical X-ray images: Hybrid generative-discriminative approach," *IET Image Process.*, vol. 7, no. 5, pp. 523–532, 2013.

[28] X. Zhang, J. Sun, S. Lu, and G. Wang, "Non-parametric detector in non-homogeneous clutter environments with knowledge-aided permutation test," *IET Radar, Sonar Navigat.*, vol. 10, no. 7, pp. 1310–1318, 2016.

[29] Z. Zhou, Y. Wang, Q. M. J. Wu, C.-N. Yang, and X. Sun, "Effective and efficient global context verification for image copy detection," *IEEE Trans. Inf. Forensics Security*, vol. 12, no. 1, pp. 48–63, Jan. 2017.

[30] Y. Masuda, T. Tateyama, W. Xiong, J. Zhou, M. Wakamiya, S. Kanasaki, A. Furukawa, and Y. W. Chen, "Liver tumor detection in CT images by adaptive contrast enhancement and the EM/MPM algorithm," in *Proc. 18th IEEE Int. Conf. Image Process.*, Sep. 2011, pp. 1421–1424.

[31] M. A. M. Salem, A. Atef, A. Salah, and M. Shams, "Recent survey on medical image segmentation," in *Handbook of Research on Machine Learning Innovations and Trends*, vol. 4, no. 1. Hershey, PA, USA: IGI Global, 2017, Ch. 19, pp. 424–464.

[32] S. Niu, Q. Chen, L. de Sisternes, Z. Ji, Z. Zhou, and D. L. Rubin, "Robust noise region-based active contour model via local similarity factor for image segmentation," *Pattern Recognit.*, vol. 61, pp. 104–119, Jan. 2017.

[33] J. Lie, M. Lysaker, and X.-C. Tai, "A piecewise constant level set framework," *Int. J. Numer. Anal. Model.*, vol. 2, no. 4, pp. 422–438, 2005.

[34] K. P. Bennett and E. J. Bredensteiner, "Duality and geometry in SVM classifiers," in *Proc. ICML*, Jun. 2000, pp. 57–64.

[35] M. Maier and R. Rannacher, "A duality-based optimization approach for model adaptivity in heterogeneous multiscale problems," *Multiscale Model. Simul.*, vol. 16, no. 1, pp. 412–428, 2018.

[36] R. E. Walpole, R. H. Myers, S. L. Myers, and K. Ye, *Probability and Statistics for Engineers and Scientists*. London, U.K.: Pearson, 2014.

[37] *The BIDMC Congestive Heart Failure Database*. Accessed: Jan. 14, 2019. [Online]. Available: https://physionet.org/physiobank/database/chfdb/

GAMAL G. N. GEWEID has a solid background in physics, mathematics, biology, radiology and imaging sciences, and strong programming skills in MATLAB, Python, and C++ programming Languages. He has a record of research publications and has excellent oral and written English communication skills. He has extensive experience working with Electronic health records (EHRs). He used patient information to improve the ability to diagnose diseases and reduce-even prevent-medical errors leading to improved patient outcomes. He has a record of research publications and four patents (surgical and diagnostic devices), all in the field of biomedicine. He applied all of them to the real patients. He also has experience and interest in using deep-learning, machine-learning, bioinformatics, signal processing in epidemiology, and other relevant topics. He is currently a Postdoctoral Research Fellow with the Electrical Engineering Department, School of Electrical Engineering and Computer Science, University of North Dakota, Grand Forks, ND, USA. He is also a very strong and professionally sound academic background in digital image processing, signal processing, multimodality medical imaging (Ultrasound, PET/CT, and MRI), CT image reconstruction, nano-robots in medicine, high-resolution MR imaging, mechatronics, medical robotics, biomedical instrumentation, computer vision, pattern recognition, software reliability and modeling, biosensors, imaging, and information technology in biomedicine. He is also involved in developing novel high resolution and fast imaging methods for neurological diseases, developing diagnostic tools, establishing risk stratification algorithms, and developing new tools for detecting chronic diseases in early stages.

MAHMOUD A. ABDALLAH received the Ph.D. degree in systems engineering from The University of Toledo, Toledo, OH, USA, in 1986. He is currently a Professor of manufacturing engineering with Central State University, Wilberforce, OH, USA. His research interests include image and signal processing, space-time adaptive processing (STAP), multiscale image compression, pattern recognition, machine learning, artificial intelligence and expert system applications in diagnostic systems, multi joint manipulators design and control, and imbedded systems. He is also a licensed Professional Engineer (PE) by the State of Ohio.